
Part Two

Physical
Processes in
Oceanography

8

Small-Scale Mixing Processes

J. S. Turner

8.1 Introduction

Forty years ago, the detailed physical mechanisms responsible for the mixing of heat, salt, and other properties in the ocean had hardly been considered. Using profiles obtained from water-bottle measurements, and their variations in time and space, it was deduced that mixing must be taking place at rates much greater than could be accounted for by molecular diffusion. It was taken for granted that the ocean (because of its large scale) must be everywhere turbulent, and this was supported by the observation that the major constituents are reasonably well mixed. It seemed a natural step to define eddy viscosities and eddy conductivities, or mixing coefficients, to relate the deduced fluxes of momentum or heat (or salt) to the mean smoothed gradients of corresponding properties. Extensive tables of these mixing coefficients, K_M for momentum, K_H for heat, and K_S for salinity, and their variation with position and other parameters, were published about that time [see, e.g., Sverdrup, Johnson, and Fleming (1942, p. 482)]. Much mathematical modeling of oceanic flows on various scales was (and still is) based on simple assumptions about the eddy viscosity, which is often taken to have a constant value, chosen to give the best agreement with the observations. This approach to the theory is well summarized in Proudman (1953), and more recent extensions of the method are described in the conference proceedings edited by Nihoul (1975).

Though the preoccupation with finding numerical values of these parameters was not in retrospect always helpful, certain features of those results contained the seeds of many later developments in this subject. The lateral and vertical mixing coefficients evaluated in this way differ by many orders of magnitude, and it was recognized that the much smaller rates of vertical mixing must in some way be due to the smaller scale of the vertical motions. Qualitatively, it was also known that the vertical eddy coefficients tended to be smaller when the density gradients were larger. The analysis of Taylor (1931) had shown that in very stable conditions K_S was smaller than K_M , which he interpreted to mean that the vertical transport of salt requires an intimate mixing between water parcels at different levels, whereas momentum can be transported by wave motion and is less affected by a strong vertical density gradient.

In contrast to these direct considerations of vertical mixing, Iselin (1939a) introduced the far-reaching idea that, because of the vertical stability, virtually all the large-scale mixing in the ocean might be accounted for in terms of lateral mixing (along isopycnals, rather than horizontally). In particular, he pointed to the striking similarity of the T - S relations for a vertical section and a surface section in the North Atlantic, each of which crossed the same isopycnals.

A strong constraint on achieving a fuller understanding of the small-scale mixing processes implicit in early measurements, was the lack of suitable instruments to resolve the scales that are directly involved. Most of the data came from water-bottle samples and widely spaced current meters, and it was tacitly assumed that the smooth profiles drawn through the discrete points actually represented the state of the ocean. Even when continuous temperature profiles became available in the upper layers of the ocean through the development of the bathythermograph, there was a tendency to attribute abrupt changes in slope to malfunctions in the instrument. The parameterization in terms of eddy coefficients implied that turbulence is distributed uniformly through depth, and is maintained by external processes acting on a smaller scale than the flows of interest; but in the absence of techniques to observe the fluctuations, and how they are maintained, little progress could be made.

Many such instruments are already in existence (see chapter 14); their use has rapidly transformed our view of the ocean, and in particular the understanding of the nature of the mixing processes. Temperature, salinity, and velocity fluctuations can be measured down to centimeter scales, and these records show that the distribution of properties is far from smooth. Rapid changes of vertical gradients are common, amounting in many cases to "steps" in the profiles. At some times the temperature and salinity variations are nearly independent, while at others they are closely correlated in a manner that has a profound effect on the vertical fluxes of the two properties (see Section 8.4.2). Viewed on a small scale, the ocean is *not* everywhere turbulent: on the contrary, turbulence in the deep ocean occurs only intermittently and in patches (which are often thin, and elongated horizontally), while the level of fluctuations through most of the volume is very low for most of the time. This is now more clearly recognized to be a consequence of the stable density gradient, which can limit the vertical extent of mixing motions and thus keep the relevant Reynolds numbers very small.

The newly acquired ability to study various mixing processes in the ocean has produced a corresponding increase in activity by theoretical and laboratory modelers in this field. The stimulation has been in both directions: theoreticians have been made aware of striking new observations requiring explanation, and they have developed more and more sophisticated theories and experiments that in turn suggest new observations to test them. Some of the work has required subtle statistical analysis of fluctuating signals, while many of the most exciting developments have been based on identifying individual mixing events (in the laboratory or the ocean), followed by a recognition of their more general significance.

Perhaps the most important factor of all has been the change in attitude to observational oceanography which took place in the early 1960s. Henry Stommel in particular advocated an approach more akin to the formulation and testing of hypotheses in other experimental sciences. Experiments designed to test specific physical ideas in a limited geographical area are now commonplace; but it is easy to forget how recently such uses of ship time have replaced the earlier "expedition" approach, in which the aim was to explore as large an area as possible in a given time (chapter 14).

This chapter will concentrate on the scales of mixing in the ocean, ranging from the smallest that have been studied to those with vertical dimensions of some tens of meters. Vertical-mixing processes will be emphasized, though the effects of quasi-horizontal intrusions near boundaries and across frontal surfaces will also be considered. After a preliminary section introducing ideas that are basic to the whole subject, various mixing phenomena will be identified and discussed in turn, starting with the sea surface and continuing into the interior and finally to the bottom. The grouping of topics within each depth range will be on the basis of the physical processes on which they depend. We shall not attempt to follow the historical order of development or to discuss observations in detail. Where there is a recent good review of a topic available, the reader will be referred to it. The major aims have been to describe the interrelation between theory, observation, and laboratory experiments that has led to the present state of understanding of each process, and to identify the areas still most in need of further work.

8.2 Preliminary Discussion of Various Mechanisms

8.2.1 Classification of Mixing Processes

It is important to keep clearly in mind the various sources of energy that can produce the turbulent motions responsible for mixing in the ocean. The first useful contrast one can make is between mechanically generated turbulence, i.e., that originating in the kinetic energy of motion, by the breakdown of a shear flow for example, and convective turbulence, produced by a distribution of density that is in some sense top heavy. The latter may occur in situations that seem obviously unstable, as when the surface of the sea is cooled [section 8.3.2.(d)], or more subtly, in the interior of the ocean when only one component (salt or heat) is unstably distributed (section 8.4.2) while the net density distribution is "hydrostatically stable."

A second informative classification depends on whether the energy comes from an "external" or "internal" source. In the first case, energy put in at a boundary is used directly to produce mixing in a region extending some distance away from the source. An

example is the mixing through the upper layers of the ocean, and across the seasonal thermocline, caused by the momentum and heat transfers from the wind blowing over the surface. By "internal mixing" is implied a process in which the turbulent energy is both generated and used in the same volume of fluid, which is in the interior well away from boundaries. The mechanisms whereby the energy is ultimately supplied to the interior region must then also be considered carefully. Reviews of mixing processes based on the above classifications or a combination of them have been given by Turner (1973a,b) and Sherman, Imberger and Corcos (1978).

8.2.2 Turbulent Shear Flows

The maintenance of turbulent energy in a shear flow will be introduced briefly by summarizing the results for a "constant stress layer" in a homogeneous fluid flowing over a fixed horizontal boundary. [For a fuller treatment of this subject see chapter 17 and Turner (1973a, chapter 5).]

The boundary stress τ_0 is transmitted to the interior fluid by the so-called Reynolds stresses $\overline{\rho u' w'}$, which arise because of the correlation between the horizontal and vertical components of turbulent velocity u' and w' . The velocity gradient responsible for maintaining the stress can be related to the "friction velocity" u_* defined by $\tau_0 = \rho u_*^2$ ($= -\overline{\rho u' w'}$ in a constant stress layer) using dimensional arguments:

$$\frac{du}{dz} = \frac{u_*}{kz}, \quad (8.1)$$

where z is the distance from the boundary and k a universal constant (the von Karman constant: $k = 0.41$ approximately). Integrating (8.1) leads to the well-known logarithmic velocity profile, which for an aerodynamically rough boundary becomes

$$u = \frac{u_*}{k} \ln \frac{z}{z_0}, \quad (8.2)$$

where z_0 , the roughness length, is related to the geometry of the boundary.

Using (8.1), one can also find the rate of production of mechanical energy per unit mass, ϵ say (which is equal to the rate of dissipation in a locally steady state):

$$\epsilon = u_*^2 \frac{du}{dz} = \frac{u_*^3}{kz}. \quad (8.3)$$

It is also possible to define an eddy viscosity

$$K_M \equiv \frac{\tau_0}{\rho} \frac{du}{dz}, \quad (8.4)$$

which is equal to ku_*z for the logarithmic profile. The relation between the flux and the gradient of a passive

tracer can in some circumstances be predicted by assuming that the turbulent diffusivity (say K_H for heat) is equal to K_M : this procedure makes use of "Reynolds analogy." Notice, however, that the assumption of a constant value of K_M or K_H , by analogy with laminar flows, is already called into question by the above analysis. The logarithmic profile implies that these coefficients are proportional to the distance z from the boundary. In practice they can turn out to be more complicated functions of position, if observations are interpreted in these terms.

8.2.3 Buoyancy Effects and Buoyancy Parameters

As already outlined in section 8.1, vertical mixing in the ocean is dominated by the influence of the (usually stable) density gradients that limit vertical motions. The dynamic effect of the density gradient is contained in the parameter

$$N = \left(-\frac{g}{\rho_0} \frac{\partial \rho}{\partial z} \right)^{1/2}, \quad (8.5)$$

the Brunt-Väisälä or (more descriptively) the *buoyancy frequency*, which is the frequency with which a displaced element of fluid will oscillate. The corresponding periods $2\pi/N$ are typically a few minutes in the thermocline, and up to many hours in the weakly stratified deep ocean.

In a shear flow, the kinetic energy associated with the vertical gradient of horizontal velocity du/dz has a destabilizing effect, and the dimensionless ratio

$$Ri = N^2 / \left(\frac{du}{dz} \right)^2 = -g \frac{d\rho/dz}{\rho_0} \left(\frac{du}{dz} \right)^2, \quad (8.6)$$

called the *gradient Richardson number*, gives a measure of the relative importance of the stabilizing buoyancy and destabilizing shear. Of more direct physical significance is the *flux Richardson number* Rf , defined as the ratio of the rate of removal of energy by buoyancy forces to its production by shear. It can be expressed as

$$Rf = \frac{g \overline{\rho' w'}}{\rho u_*^2 (du/dz)} = \frac{K_H}{K_M} Ri \quad (8.7)$$

where ρ' is the density fluctuation and $B = -g \overline{\rho' w'} / \bar{\rho}$ is the buoyancy flux. Note that K_H may be much smaller than K_M in a stratified flow, so that while there is a strict upper limit of unity for Rf in steady conditions with stable stratification, turbulence can persist when $Ri > 1$.

Another "overall" Richardson number expressing the same balance of forces, but involving finite differences rather than gradients, can be written in terms of the overall scales of velocity u and length d imposed by the boundaries:

$$Ri_0 = g \frac{\Delta\rho}{\rho} d / u^2. \quad (8.8)$$

One must always be careful to define precisely what is meant when this term is used.

Two parameters commonly used to compare the relative importance of mechanical and buoyancy terms are expressed in the form of lengths. When the vertical fluxes of momentum $\tau_0 = \rho u_*^2$ and buoyancy B are given, then the Monin-Obukhov length (Monin and Obukhov, 1954)

$$L = \frac{-u_*^3}{kB} \quad (8.9)$$

(where k is the von Karman constant defined in (8.1) is a suitable scaling parameter; it is negative in unstable conditions and positive in stable conditions. This is a measure of the scale at which buoyancy forces become important; as B becomes more negative (larger in the stabilizing sense) buoyancy affects the motions on smaller and smaller scales. If, on the other hand, the rate of energy dissipation ϵ and the buoyancy frequency are known, then dimensional arguments show that the length scale

$$L_0 = \epsilon^{1/2} N^{-3/2}, \quad (8.10)$$

first used by Ozmidov (1965), is the scale of motion above which buoyancy forces are dominant.

The molecular diffusivity κ (of heat, say) and kinematic viscosity ν do not appear in the parameters introduced above (though the processes of dissipation of energy and of buoyancy fluctuations ultimately depend on molecular effects at the smallest scales [section 8.4.1(d)]. When convectively unstable conditions are considered, however, the relevant balance of forces is between the driving effect of buoyancy and the stabilizing influence of the two diffusive processes that act to retard the motion. The parameter expressing this balance, the Rayleigh number

$$Ra = g \frac{\Delta\rho}{\rho} d^3 / \kappa\nu \quad (8.11)$$

does therefore involve κ and ν explicitly. Here $\Delta\rho/\rho = \alpha\Delta T$ is the fractional (destabilizing) density difference between the top and bottom of a layer of fluid of depth d (often due to a temperature difference ΔT , where α is the coefficient of expansion). The Reynolds number $Re = ud/\nu$ and the Prandtl number $Pr = \nu/\kappa$ can also be relevant parameters in both the stable and convectively unstable cases. In particular, it is clear that the Reynolds number based on internal length scales such as (8.9) and (8.10) is much smaller than that defined using the whole depth, which would only be appropriate if the ocean were homogeneous.

8.2.4 Turbulent Mixing and Diffusion in the Horizontal

We mention now several ideas which will not be followed up in detail in this review but which have had an important effect on shaping current theories of mixing in the ocean.

Eckart (1948) pointed to the distinction which should be made between stirring and mixing processes. The former always increase the gradients of any patch of marker moving with the fluid, as it is sheared out by the larger eddies of the motion. True mixing is only accomplished when molecular processes, or much smaller-scale turbulent motions, act to decrease these gradients and spread the marker through the whole of the larger region into which it has been stirred.

The total range of eddy scales, up to that characteristic of the current size of the patch, also play a part in the "neighbor separation" theory of diffusion due to Richardson (1926), which was originally tested in the atmosphere, and applied to the ocean by Richardson and Stommel (1948). Their results imply that the separation of pairs of particles l or equivalently the dispersion $\Sigma = \overline{y^2}$, of a group of particles about its center of gravity, satisfies a relation of the form

$$\frac{\partial\Sigma}{\partial t} \propto \Sigma^{2/3} \propto l^{4/3}. \quad (8.12)$$

The rate of separation and hence the effective diffusivity increases with increasing scale because a larger range of eddy sizes can act on the particles. As Stommel (1949) pointed out, there is no way that (8.12) can be reconciled with an ordinary gradient (Fickian) diffusion theory using a constant eddy diffusivity. He showed, however, that it is explicable using Kolmogorov's theory of the inertial subrange of turbulence. Ozmidov (1965) has demonstrated that (8.12) can be written down directly using a dimensional argument, assuming that the rate of change of Σ (which has the same dimensions as an eddy diffusivity) depends only on the value of Σ and the rate of energy dissipation ϵ :

$$\frac{\partial\Sigma}{\partial t} \propto \epsilon^{1/3} \Sigma^{2/3}. \quad (8.12a)$$

Bowden (1962) summarized the evidence available up to that time to show that this $\Sigma^{2/3}$ (or $l^{4/3}$) relation described the observations well over a wide range of scales, from 10 to 10^8 cm. The dependence on ϵ was not then investigated explicitly, but later experiments have shown that this factor (and hence the rate of diffusion) can vary greatly with the depth below the surface.

The apparent "longitudinal diffusion" produced by a combination of vertical (or lateral) shear and transverse turbulent mixing is another important concept. This originated in a paper by Taylor (1954), who showed that the downstream extension of a cloud of

marked particles due to shear, followed by cross-stream mixing, leads to much larger values of the longitudinal dispersion coefficient D than can be produced by turbulence alone. For homogeneous fluid in a two-dimensional channel it is given by

$$D = 5.9du_* \quad (8.13)$$

where d is the depth and u_* the friction velocity.

Fischer (1973, 1976) has written two excellent reviews of the application of these (and other) results to the interpretation of diffusion processes in open channels and estuaries. The second in particular contains much that is of direct interest to oceanographers (cf. chapter 7).

8.3 Vertical Mixing in the Upper Layers of the Ocean

The major inputs of energy to the ocean come through the air-sea interface, and it is in the near-surface layers that the concept of an "external" mixing process is most clearly applicable. Because of the overall static stability, the direct effects of the energy input is to produce a more homogeneous surface layer, with below it a region of increased density gradient. Thus one must consider in turn the nature of the energy sources at the surface (whether the mixing is due to the mechanical effect of the wind stress, or to the transfer of heat), the influence of these on the motion in the surface layer, and finally the mechanism of mixing across the thermocline below. The variation of these processes with time, which leads to characteristic daily or seasonal changes of the thermocline, will also be considered. Most of the models are one-dimensional in depth, implying that the mixing is uniform in the horizontal, but some individual localized mixing processes will be discussed (see chapter 9 for additional discussion).

8.3.1 Parameterization of Stratified Shear Flows

The earliest theories of flow driven by the stress of the wind acting on the sea surface were based on an extension of the eddy-viscosity assumption. The vertical transports of heat and momentum can be related to the mean gradients of these properties using eddy coefficients that have an assumed dependence on the stability. Munk and Anderson (1948), for example, took K_H and K_M to be particular (different) functions of the gradient Richardson number (8.6), assumed that the (stabilizing) heat flux was constant through the depth, and solved the resultant closed momentum equation numerically to derive the velocity and temperature profiles. More recently, this method has been taken up again, but using more elaborate second-order closure schemes to produce a set of differential equations for the mean fields and the turbulent fluxes in the vertical (see, e.g., Mellor and Durbin, 1975; Launder, 1976; Lumley, 1978).

In this writer's opinion, this method has not yet proved its value for stratified flows in the ocean. The method is relatively complex, and the necessary extrapolations from known flows are so hard to test that the integral methods described in the following sections are at present preferred because they give more direct physical insight. It will, however, be worth keeping in touch with current work in this rapidly developing field.

8.3.2 Mixed-Layer Models

Thorough reviews of the various one-dimensional models of the upper ocean that have appeared (mainly in the past 10 years) have been given by Niiler (1977), and Niiler and Kraus (1977) [and the whole volume edited by Kraus (1977) is very useful]. The treatment here will be more selective: certain features of the models will be isolated, and their relative importance assessed. Laboratory experiments that have played an important role in the development of these ideas will also be discussed (though these have not always proved to be as directly relevant as was originally thought).

The starting point of all these models, which is based on many observations in the ocean and the laboratory, is that the mean temperature and salinity (and hence the density) are nearly uniform within the surface layer. In the case where mixing is driven by the action of the wind stress at the surface, the horizontal velocity in this layer is also assumed to be constant with depth, implying a rapid vertical exchange of horizontal momentum throughout the layer. Another assumption used in most theories is that there is an effectively discontinuous change of these variables across the sea surface and across the lower boundary of the mixed layer (see figure 8.1).

It is implied in what follows that the surface mixing is limited by buoyancy effects, not by rotation (i.e., the "Ekman layer depth" v_* / f is not a relevant scale), but rotation still enters into the calculation of the velocity step across the interface (see section 8.3.3). The Ekman layer depth will be considered explicitly in the context of bottom mixing (section 8.5.1).

Integration of the conservation equations for the heat (or buoyancy) content, and the horizontal momentum equation (in rotating coordinates where appropriate) across such a well-mixed layer, gives expressions for the temperature and bulk horizontal velocity in terms of the exchanges of heat and momentum across the sea surface and the interface below. The surface fluxes are in principle calculable from the external boundary conditions, but the interfacial fluxes are not known a priori. They depend on the rate of deepening, i.e., the rate at which fluid is mixed into the turbulent layer from the stationary region below. A clear understanding of the mechanism of *entrainment* across a density interface, with various kinds of mechanical or convec-

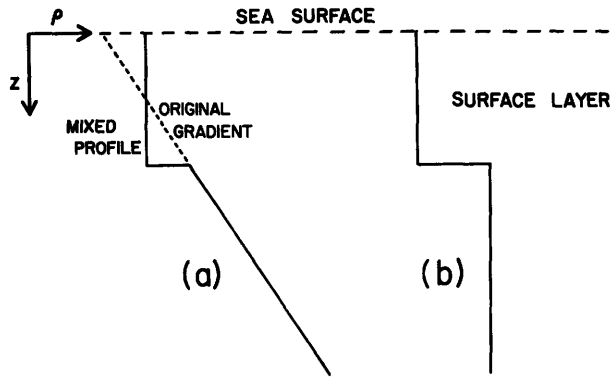


Figure 8.1 Sketch of the two types of density profiles discussed in the text: (a) a well-mixed surface layer with a gradient below it, (b) a two-layer system, with homogeneous water below.

tive energy inputs near the surface, is therefore a crucial part of the problem.

(a) Mixing Driven by a Surface Stress Purely mechanical mixing processes will be discussed first, starting with the case where a constant stress $\tau_0 = \rho_w v_*^2$ is applied at the surface (for example, by the wind), without any transfer of heat. When the water is stratified, a well-mixed layer is produced (see figure 8.1), which at time t has depth h and a density step below it, $\Delta\rho$ say. A dimensional argument suggests that the entrainment velocity $u_e = dh/dt$ can be expressed in the form

$$E_* = \frac{u_e}{v_*} = E_*(Ri_*) \quad (8.14)$$

where

$$Ri_* = \frac{g \Delta\rho h}{\rho_w v_*^2} = \frac{C^2}{v_*^2} \quad (8.15)$$

is an overall Richardson number based on the friction velocity v_* in the water. For the moment dh/dt is taken to be positive, but the general case where h can decrease will be considered in section 8.3.2(d).

Two related laboratory experiments have been carried out to model this process and test these relations. Kato and Phillips (1969) started with a linear salinity gradient (buoyancy frequency N) and applied a stress τ_0 at the surface (figure 8.1a). The depth h of the surface layer is related to $\Delta\rho$ and N by

$$C^2 = g \frac{\Delta\rho}{\rho} h = \frac{1}{2} N^2 h^2 \quad (8.16a)$$

Kantha, Phillips, and Azad (1977) used the same tank (annular in form, to eliminate end effects), but filled it with two layers of different density (figure 8.1b) rather than a gradient. In this case, conservation of buoyancy gives

$$C^2 = g \frac{\Delta\rho}{\rho} h = a \text{ constant.} \quad (8.16b)$$

Thus C^2 and Ri_* are clearly increasing as the layer deepens in the first case (8.16a) whereas they are constant when (8.16b) holds.

Equation (8.14) does not, however, collapse the data of these two experiments onto a single curve: at a given Ri_* and h , E_* was a factor of two larger in the two-layer experiment than with a linear gradient. Price (1979) has proposed that the rate of entrainment should be scaled instead with the mean velocity V of the layer (or more generally, the velocity difference across the interface):

$$\frac{u_e}{V} = E(Ri_V) \quad (8.17)$$

where Ri_V is also defined using V . This is a more appropriate way to describe the process, since other physical effects may intervene between the surface and the interface and V need not be proportional to v_* . (In the experiments described above, side wall friction can dominate, though the method used to correct for this will not be discussed explicitly here.)

The form of Ri_V deduced from the experiments agrees with that previously obtained by Ellison and Turner (1959), which is shown in figure 8.2. [This will also be discussed in another context in section 8.5.2(a).] For the present purpose, we note only that E falls off very rapidly between $0.4 < Ri_V < 1$, so that $Ri_V \approx 0.6$ is a good approximation for Ri_V over the whole range of experimental results. The *assumption* that Ri_V is constant (which was based on an argument about the stability of the layer as a whole) was made by Pollard, Rhines, and Thompson (1973). This was used as the basis of the closure of their mixed-layer model which will be referred to in section 8.3.3.

The formulation in terms of V implies that conservation of momentum is the most important constraint

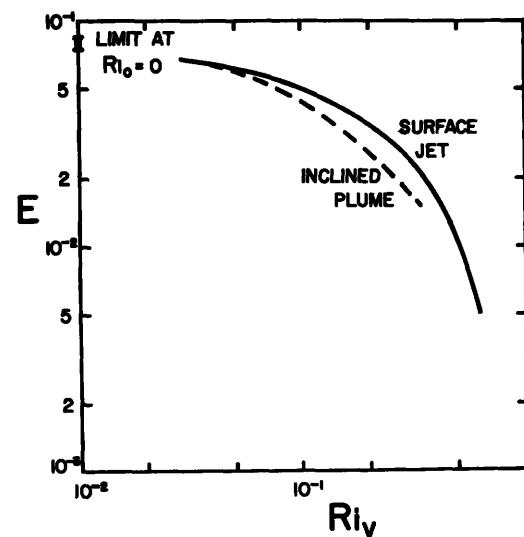


Figure 8.2 The rate of entrainment into a turbulent stratified flow as a function of overall Richardson number, for two types of experiments described by Ellison and Turner (1959).

on the entrainment in these laboratory experiments (and in the analogous oceanic case). The momentum equation

$$\frac{d(hV)}{dt} = v_*^2 = \text{constant}, \quad (8.18)$$

together with the conservation of buoyancy relations (8.16), gives

$$E_* = \frac{u_e}{v_*} = n Ri_v^{1/2} Ri_*^{-1/2} \quad (8.19)$$

where

$$n = \begin{cases} \frac{1}{2} & \text{if } C^2 = \frac{1}{2} N^2 h^2 \text{ (linear stratification)} \\ 1 & \text{if } C^2 = \text{constant (homogeneous lower layer)}. \end{cases}$$

The predicted entrainment rate is a factor of two smaller in the linearly stratified case, as is observed. This difference arises because, in order to maintain Ri_v constant as C^2 increases, the whole layer, as well as the entrained fluid, must be accelerated to a velocity $V = (C^2/Ri_v)^{1/2}$. In the two-layer case, the stress is only required to accelerate entrained fluid to velocity V , which is constant.

Nothing has been said yet about the detailed mechanism of mixing across the interface, in the laboratory or in the ocean. Thorpe (1978a) has shown from measurements in a lake under conditions of surface heating that Kelvin-Helmholtz instability dominates the structure soon after the onset of a wind [section 8.4.1(c)]. Dillon and Caldwell (1978) have demonstrated the importance of a few "catastrophic events," relative to the much slower continuous entrainment processes. We tentatively suggest that these events could be the breakdown of large-scale waves on the interface, a mechanism that has been proposed for the benthic boundary layer (see section 8.5.1).

(b) The Influence of Surface Waves The experiments just described, and the models based on them, imply that the whole effect of the wind stress on the surface is equivalent to that produced by a moving plane, solid boundary. There is only one relevant length scale, the depth of the well-mixed layer. In the ocean, of course, there is a free surface on which waves are generated as well as a current, and this can introduce entirely new physical effects. The presence of waves can modify the heat, momentum, and energy transfer processes [as reviewed by Phillips (1977c)] and individual breaking waves can inject turbulent energy at a much smaller scale. Longuet-Higgins and Turner (1974) and Toba, Tokuda, Okuda, and Kawai (1975) have taken the first steps toward extending wave theories into this turbulent regime.

The interaction between a wind-driven current and surface waves can produce a system of "Langmuir

cells," aligned parallel to the wind. These circulations, extending through the depth of the mixed layer, have long been recognized to have a significant effect on the mixing, and there are many theories purporting to explain the phenomenon [see Pollard (1977) for a review]. It now appears most likely that the generation depends on an instability mechanism, in which there is a positive feedback between the wind-driven current and the cross-wind variation in the Stokes drift associated with an intersecting pattern of two crossed wave trains. Physically, this implies that the vorticity of the shear flow is twisted by the presence of the Stokes drift into the vorticity of the Langmuir circulations. A heuristic model of the process was given by Garrett (1976), but the most complete and satisfactory theory is that of Craik (1977), who has clarified the differences between earlier related models. Faller (1978) has carried out preliminary laboratory experiments that support the main conclusions of this analysis (see also chapter 16).

The effect of density gradients on these circulations has not yet been investigated, so it is not clear whether a mixed layer can be set up by this mechanism under stable conditions. At high wind speeds, however, it seems likely that these organized motions, with horizontal separation determined by the wave field, will have a major influence on both the formation and rate of deepening of the mixed layer. This is an important direction in which the detailed modeling of thermocline mixing processes should certainly be extended.

(c) Input of Turbulent Energy on Smaller Scales The case where kinetic energy is produced at the surface, with turbulence scales much less than that of the mixed layer, has been modeled in the laboratory using an oscillating grid of solid bars. An early application to the ocean was made by Cromwell (1960). The more recent experiments by Thompson and Turner (1975), Hopfinger and Toly (1976), and McDougall (1979), have shown that the turbulent velocity decays rapidly with distance from the grid (like z^{-1}), while its length scale l is proportional to z . The experiments also suggest that the entrainment across an interface below is most appropriately scaled in terms of the velocity and length scales u_1 and l_1 of the turbulence near the interface, rather than using overall parameters such as the velocity of the stirrer and the layer depth. When this is done, the laboratory data are well-described by the relation

$$\frac{u_e}{u_1} = f(Ri_0, Pe), \quad (8.20)$$

where

$$Ri_0 = \frac{g \Delta \rho}{\rho} \frac{l_1}{u_1^2},$$

$Pe = u_1 l / \kappa$ is a Peclet number.

The general form of the curves is similar to those shown in figure 8.2, but there is a distinct difference between the results of experiments using heat and salt as the stratifying agent (reflecting the different molecular diffusivity κ in Pe). They tend to the same form with a small slope at low Ri_0 , where neither buoyancy nor diffusion is important, but diverge at larger Ri_0 to become approximately $u_e/u_1 \propto Ri_0^{-1}$ (heat) and $u_e/u_1 \propto Ri_0^{-3/2}$ (salt). The first form is attractive since it seems to correspond to the prediction of a simple energy argument (see Turner 1973a, chapter 9), but it now appears that one must accept the complications of the general form (8.20), including the fact that molecular processes can affect the structure of the interface and hence the entrainment at low values of Pe (Crapper and Linden, 1974).

The laboratory experiments of Linden (1975) have also shown that the rate of entrainment across an interface, due to stirring with a grid, can be substantially reduced when there is a density gradient below, rather than a second homogeneous layer. This is due to the generation, by the interfacial oscillations, of internal gravity waves that can carry energy away from the interface. The process can have a substantial effect on the mixing in the thermocline below the sharp "interface" itself. It is also a source of wave energy for the deep ocean, though the existence of a mean shear flow in the upper layer probably has an important influence on wave generation as well as on wave breaking (Thorpe, 1978b). It seems likely too that the process of mixing itself is affected in a significant way by the presence of a mean shear. Certainly organized motions in the form of Kelvin-Helmholz billows occur only with a shear [see section 8.4.1(c)].

(d) The Effect of a Surface Heat Flux Only mechanical energy inputs have so far been considered; the effect of a buoyancy flux will now be added. The discussion will be entirely in terms of heat fluxes, but clearly the increase in salinity due to evaporation should also be taken into account (see, e.g., Niiler and Kraus, 1977).

When there is a net (equivalent) heat input to the sea surface, a stabilizing density gradient is produced that has an inhibiting effect on mixing. Note, however, that penetrating radiation, with simultaneous cooling by evaporation and long-wave radiation right at the surface, produces a localized convective contribution to the turbulence (see Foster, 1971). When there is a net cooling, at night or in the winter, convective motions can extend through the depth of the mixed layer and contribute to the entrainment across the thermocline below. In the latter case, detailed studies of the heat transfer and the motions very near the free surface have been carried out by Foster (1965), McAlister and McLeish (1969) and Katsaros et al. (1977) for example, and a comparison between fresh and salt water has

recently been made by Katsaros (1978).

When there is a constant stabilizing buoyancy flux $B = g\overline{\rho'w'}/\bar{\rho}$ from above (i.e., a constant rate of heating, assumed to be right at the surface), and simultaneously a fixed rate of supply of kinetic energy, there can be a balance between the energy input and the work required to mix the light fluid down. Assuming, as did Kitaigorodskii (1960), that the friction velocity u_* is the parameter determining the rate of working, the depth of the surface layer can become steady at

$$h = au_*^3/B \quad (8.21)$$

while it continues to warm. This argument is closely related to that leading to the Monin-Obukhov length (8.9), and is also a statement of the conservation of energy.

During periods of increasing heating, the equilibrium depth achieved will be continually decreasing, so that the bottom of the mixed layer will rise and leave previously warmed layers behind. The minimum depth coincides with the time of maximum heating (assuming a constant rate of mechanical stirring). As the rate of heating decreases, the interface will descend slowly, while the temperature of the upper layer increases. Finally, when the surface is being cooled, there will be a more rapid cooling and also a deepening of the upper layer. Whether this mixing is "penetrative" or "non-penetrative," i.e., the extent to which convection contributes to entrainment across the thermocline, is the subject of a continuing debate that is summarized in the following section. Molecular effects can also affect the rate of entrainment at low Pe , by altering the shape of the density profile on which the convective turbulence acts.

8.3.3 Energy Arguments Describing the Behavior of the Thermocline

Virtually all the models of the upper mixed layer in current use are based on energy arguments that balance the inputs of kinetic energy against changes in potential energy plus dissipation. They vary in the emphasis they put on different terms in the conservation equations, but some of the conflict between alternative models is resolved by recognizing that different processes may dominate at various stages of the mixing.

Niiler (1975) and de Szoeke and Rhines (1976), for instance, have shown that four distinct dynamic stages can be identified in the case where a wind stress begins to blow over the surface of a linearly stratified ocean (assuming there is no heating or energy dissipation). Using standard notation, the turbulent kinetic energy equation can then be summarized as

$$\frac{1}{2} \frac{\partial h}{\partial t} \left(\begin{array}{ccc} \alpha u_*^2 & + \frac{N^2 h^2}{2} & - |\delta V|^2 \\ A & B & C \end{array} \right) = \begin{array}{c} m u_*^3 \\ D \end{array} \quad (8.22)$$

The terms represent

- A the storage rate of turbulent energy in the mixed layer;
- B the rate of increase of potential energy due to entrainment from below;
- C the rate of production of turbulent mechanical energy by the stress associated with the entrainment across a velocity difference δV ;
- D the rate of production of turbulent mechanical energy by surface processes.

Initially, there is a balance between *A* and *D* and the depth of the layer grows rapidly to a meter or so. After a few minutes, a balance between *B* and *D* is attained, and the mixed layer under typical conditions can grow to about 10 meters within an hour. In the meantime, the mean flow has been accelerating, and the velocity difference across the base of the layer increasing. Following Pollard et al. (1973), it can be deduced from the momentum equations in rotating coordinates that

$$(\delta V)^2 = \frac{2u_*^4}{h^2 f^2} [1 - \cos(ft)], \quad (8.23)$$

where *f* is the Coriolis parameter. The turbulent energy produced at the base of the mixed layer by this shear can dominate on a time scale of half a pendulum day, and the balance is between *B* and *C*. The depth after this time is of order $u_*/(Nf)^{1/2}$, determined both by the stratification and rotation. [A modification of this argument by Phillips (1977b) leads to the alternative form $u_*/f^{2/3}N^{1/3}$, but observationally it could be difficult to choose between them.] In order to close this model, one still needs to add an independent criterion to relate the entrainment to the shear across the interface. As discussed in section 8.3.2(a), this can be taken as $Ri_v \approx 0.6$ since the mixing rate falls off sharply at this value of the overall Richardson number.

Finally, the intensity of the inertial currents decreases and a slow erosion continues, again as a balance between *B* and *D*. It is this final state that corresponds to the model of the seasonal thermocline introduced by Kraus and Turner (1967), and modified by Turner (1973b). Without considering any horizontal motion, they used the one-dimensional heat and mechanical energy equations, assuming that all the kinetic energy is generated at the surface, and that a constant fraction of this is used for entrainment across the interface below. This model can also deal with the case where the surface is being heated. Gill and Turner (1976) have carried the discussion a stage further, and shown that the cooling period is much better described by assuming that the convectively generated energy is nonpenetrative, i.e., that it contributes very little to the entrainment, only to the cooling of the layer.

As will be apparent from the earlier discussion of individual mixing mechanisms, it is by no means easy

to identify which sources of energy are important, much less to quantify their effects. The most arbitrary feature of mixed-layer models at present is the parameterization of dissipation. It is usually assumed (or implied) that the energy available for entrainment is some fixed fraction of that produced by each type of source, and laboratory and field data are used to evaluate the constants of proportionality. This is the view adopted in the review by Sherman et al. (1978), for example, who added a term representing radiation of wave energy from the base of the layer. They compared the coefficients chosen by various authors, as well as suggesting their own best fit to laboratory experimental data. Another such comparison with laboratory and field data has been made by Niiler and Kraus (1977).

Processes such as the decay of turbulent energy with depth, and the removal by waves propagating through a density gradient below, are not adequately described by such constant coefficients. It is not clear that the shear through the layer is small enough to ignore as a source of extra energy, nor that two-dimensional effects (due to small-scale intrusions in the thermocline) are unimportant. In short, the models seem to have run ahead of the physical understanding on which they should be based. In the following section, some of the theoretical predictions will be compared with observations, consisting usually only of the mixed-layer depth and temperature. There are some good measurements of fluctuating temperature and salinity (Gregg 1976a) but to make further progress, and to distinguish between alternative models, much more detailed measurements of turbulent velocity and structure through the surface mixed layer and the thermocline below will be required. Thorpe (1977) and his coworkers have made the best set of measurements to date, using a Scottish Loch as a large-scale natural laboratory. (The JASIN 1978 experiment should contribute greatly to our understanding of these processes, but none of those results were available at the time of writing.)

8.3.4 Comparison of Models and Observations

In the absence of detailed measurements, the best hope of testing theories lies in choosing simple experimental situations in which as few as possible of the competing processes are active, or where they can be clearly distinguished. It is pointless, for example, to apply a model based on surface inputs alone if the turbulent-energy generation is in fact dominated by shear at the interface.

Price, Mooers, and van Leer (1978) have reported detailed measurements of temperature and horizontal-velocity profiles for two cases of mixed-layer deepening due to storms. They estimated the surface stress from wind observations, and compared model calculations based directly on u_*^2 with those based on the velocity difference (8.23). The predicted responses are quite dif-

ferent in the two cases, and the latter agreed well with the observations. The deepening rate accelerated during the initial rise in wind stress, but decreased abruptly as δV was reduced during the second half of the inertial period, even though u_*^2 continued to increase. They thus found no evidence of deepening driven by wind stress alone on this time scale, although turbulence generated near the surface must still have contributed to keeping the surface layer stirred.

A particularly clear-cut series of observations on convective deepening was reported by Farmer (1975). He has also given an excellent account of the related laboratory and atmospheric observations and models in the convective situation. The convection in the case considered by Farmer was driven by the density increase produced by surface heating of water, which was below the temperature of maximum density in an ice-covered lake. Thus there were no horizontal motions, and no contribution from a wind stress at the surface. From successive temperature profiles he deduced the rate of deepening, and showed that this was on average 17% greater than that corresponding to "nonpenetrative" mixing into a linear density gradient. Thus a small, but not negligible, fraction of the convective energy was used for entrainment. [The numerical values of the energy ratio derived in this and earlier studies will not be discussed here; but note that the relevance of the usual definition has been called into question by Manins and Turner (1978).]

In certain well-documented cases, models developed from that of Kraus and Turner (1967) (using a parameterization in terms of the surface wind stress and the surface buoyancy flux) have given a good prediction of the time-dependent behavior of deep surface mixed layers. Denman and Miyake (1973), for example, were able to simulate the behavior of the upper mixed layer at ocean weather station P over a 2-week period. They used observed values of the wind speed and radiation, and a fixed ratio between the surface energy input and that needed for mixing at the interface.

On the seasonal time scale, Gill and Turner (1976) have systematically compared various models with observations at a North Atlantic weather ship. They concluded that the Kraus-Turner calculation, modified to remove or reduce the penetrative convective mixing during the cooling cycle, gives the best agreement with the observed surface temperature T_s of all the models so far proposed. In particular, it correctly reproduces the phase relations between the dates of maximum heating, maximum surface temperature, and minimum depth, and it predicts a realistic hysteresis loop in a plot of T_s versus total heat content H (i.e., it properly incorporates the asymmetry between heating and cooling periods). This behavior is illustrated in figure 8.3. The model also overcomes a previous difficulty and allows the potential energy to decrease during the cool-

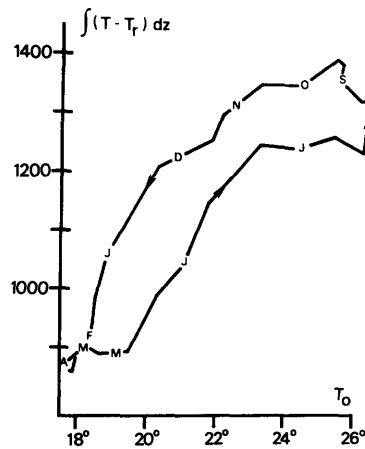


Figure 8.3 The heat content in the surface layer as a function of surface temperature T_0 at ocean weather station Echo. (After Gill and Turner, 1976.) The reference temperature T_r is the mean of the temperature at 250 m and 275 m depth, and the months are marked along the curve.

ing period, instead of increasing continuously as implied by the earlier models.

The mixed-layer depth and the structure of the thermocline are not, however, well predicted by these models; this fact points again to the factors that have been neglected. Niiler (1977) has shown that improved agreement is obtained by empirically allowing the energy available for mixing to decrease as the layer depth increases [though a similar behavior is implied by the use of (8.23); see Thompson (1976) for a comparison of the two types of model]. Direct measurements of the decay of turbulent energy with depth in the mixed layer will clearly be important. In many parts of the ocean it may also be necessary to consider upwelling.

Perhaps the most important deficiency is the neglect of any mixing below the surface layer. There is now strong evidence that the density interface is never really sharp, but has below it a gradient region that is indirectly mixed by the surface stirring. At greater depths too, the density profile is observed to change more rapidly than can be accounted for by advection, so that mixing driven by internal waves, alone or in combination with a shear flow, must become significant. These internal processes are the subject of the following section.

8.4 Mixing in the Interior of the Ocean

The overall properties of the main thermocline apparently can be described rather well in terms of a balance between upwelling w and turbulent diffusion K in the vertical. Munk (1966), for example, after reviewing earlier work, summarized data from the Pacific that show that the T and S distributions can be fitted by exponentials that are solutions of diffusion equations, for example

$$K \frac{d^2 T}{dz^2} - w \frac{dT}{dz} = 0, \quad (8.24)$$

with the scaleheight $K/w \approx 1$ km. By using distributions of a decaying tracer ^{14}C , he also evaluated a scale time K/w^2 , and the resulting upwelling velocity $w \approx 1.2 \text{ cm day}^{-1}$ and eddy diffusivity $K \approx 1.3 \text{ cm}^2 \text{ s}^{-1}$ have been judged "reasonable" by modelers of the large-scale ocean circulation (chapter 15). Munk found the upwelling velocity consistent with the quantity of bottom water produced in the Antarctic, but he was not able to deduce K using any well-documented physical model. The most likely candidate seemed to be the mixing produced by breakdown of internal waves, but other possibilities are double-diffusive processes, and quasi-horizontal advection following vertical mixing in limited regions (such as near boundaries or across fronts).

Some progress has been made in each of these areas in the past 10 years, and they will be reviewed in turn. First, however, we shall discuss a set of interrelated ideas about the energetics of the process that are vital to the understanding of all types of mixing in a stratified fluid.

8.4.1 Mechanical Mixing Processes

(a) Energy Constraints on Mixing The overall Richardson number Ri_0 [defined by equation (8.8)] based on the velocity and density differences over the whole depth of the ocean, is typically very large, implying that the associated flow is dynamically very stable. But a second important fact is that the profiles of density (and other properties) are now known to be very nonuniform, with nearly homogeneous layers separated by interfaces where the gradients are much larger. Is it possible that a discontinuous structure of this kind (figure 8.4) is less stable, allowing turbulence to exist when it could not do so in the smooth average conditions?

Part of the answer was given by Stewart (1969), whose argument was developed by Turner (1973a, chapter 10). It can be shown that nonuniform profiles (different for velocity and density) can be chosen such that any value of the gradient Richardson number is attained everywhere in the interior, whatever the value of Ri_0 —essentially because

$$(\Delta U / \Delta z)^2 \leq (\overline{\partial u / \partial z})^2. \quad (8.25)$$

Thus a redistribution of properties can always reduce the gradient Ri to a value at which turbulence can be maintained.

But a crucial question remains: how is this redistribution actually produced? Consider the energy changes associated with a transition from linear gradients of velocity and density $u = \alpha z$, $\rho = -\beta z + \rho_0$ say, to a well-mixed layer of depth H (see figure 8.4). The change

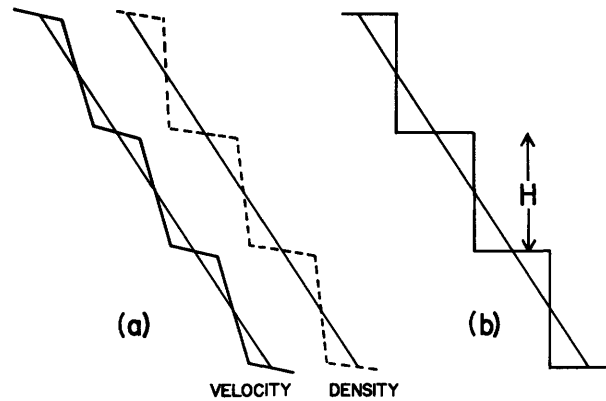


Figure 8.4 Discontinuous profiles produced by mixing, from initially linear density and velocity distributions. In (a) the final profiles, different for density and velocity, correspond to a constant gradient Richardson number everywhere, and (b) is the simpler model of homogeneous layers and thin interfaces used to derive (8.26).

in kinetic energy is $(1/24)\alpha^2 H^3$ and in potential energy $(1/12)g\beta H^3$; the two are equal when

$$Ri_0 = g\beta/\alpha^2 = 1/2. \quad (8.26)$$

This argument implies that for all $Ri_0 \gg 1$ there is not enough kinetic energy in the local mean motion to produce the observed, nonuniform profiles, even when dissipation is neglected entirely. In the absence of sources of convective energy due to double-diffusive processes (see section 8.4.2), the general conclusion is inescapable: extra energy must be propagated into the region from the boundaries in the form of inertial or internal gravity waves if mixing is to be sustained.

The role of internal waves and their relation to the nonuniform density structure may be approached in another way, using the argument set out by Turner (1973a, p. 137), and extensions of it. Consider a deep region of stable fluid, having linear profiles of both density and velocity through it. Suppose there is a constant stress (momentum flux) $\tau_0 = \rho u_*^2$ and buoyancy flux B through this region, sustained by small-scale turbulent motions. Mixing occurs only with fluid immediately above and below any level, so that only the internal lengthscale L defined by (8.9) will be relevant, not the overall depth or the distance from the boundaries. It follows on dimensional grounds that

$$\frac{du}{dz} = k_1 \frac{-B}{u_*^2} = k_1 \frac{u_*}{L}, \quad (8.27)$$

$$N^2 = -\frac{g}{\rho} \frac{d\rho}{dz} = k_2^2 \frac{B^2}{u_*^4} = k_2^2 \frac{u_*^2}{L^2} \quad (8.28)$$

where k_1 and k_2 are constants (which have not been determined experimentally). This is thus an equilibrium, self-regulated state, in which there is a unique relation between the gradients and the fluxes. The flux

Richardson number (8.7) has a fixed value $Rf = k_1^{-1}$, and so does the gradient Richardson number

$$Ri = k_2^2/k_1^2 = Ri_e, \quad (8.29)$$

which has been called the equilibrium Richardson number.

Only in rather special cases can this equilibrium state be maintained—one good example is the edge of a turbulent gravity current, which is treated in section 8.5.2. When density and velocity differences are imposed over a given depth, the only equilibrium state is $Ri_0 = Ri_e$. If $Ri_0 < Ri_e$, the shear will dominate, and mixing will soon be influenced directly by the boundaries. If $Ri_0 > Ri_e$, as it is in the case of most interest here, then the stratification will dominate, though we have already seen how a nonuniform stratification allows the local Ri to be much smaller than Ri_0 , so that turbulence can persist.

In this nonuniform state, however, (8.27) shows that the transport of momentum by turbulent processes is much less efficient in the interfaces where du/dz is larger, and it is impossible to have constant purely turbulent fluxes of both buoyancy and momentum through the whole depth. But the existence of interfacial waves provides a complementary mechanism to transport momentum across the steep gradient regions without a corresponding increase in the buoyancy flux.

There have been other suggestions about the mechanism of formation of layers from a linear gradient that can be related to the above ideas. Posmentier (1977), extending an idea formulated by Phillips (1972), suggested that if the vertical turbulent flux of buoyancy decreases as the vertical density gradient increases, any perturbation causing an increase in the gradient will be amplified. This occurs because the local decrease in flux leads to an accumulation of mass, which increases the density gradient further. This behavior is in contrast to the more familiar case, described by an eddy diffusivity, where an increase in gradient increases the flux, thus tending to smooth out any irregularity.

Linden (1979) has recently reviewed a wide range of laboratory experiments on "mechanical" mixing across a density interface, including those that use a shear flow, or stirring with oscillating grids [cf. sections 8.3.2(a) and 8.3.2(c)], and has suggested how they can be unified in terms of an energy argument. Briefly, he has shown that as the overall Richardson number Ri_0 increases from zero, the flux Richardson number Rf at first increases, reaches a maximum, and then falls as Ri_0 becomes even larger (see figure 8.5). This form can most readily be understood in terms of the grid-stirring results already described in section 8.3.2(c). The rate of increase in potential energy is $\frac{1}{2}g\Delta\rho u_e D^2$, where u_e is the entrainment velocity, and the rate of supply of kinetic energy is $\frac{1}{2}\rho u^3 D$. Thus by definition

$$Rf = \frac{u_e g \Delta\rho D}{u \rho u^2} = \frac{u_e}{u} Ri_0. \quad (8.30)$$

Using the power-law fit to the experiments $u_e/u \propto Ri_0^{-n}$, we find

$$Rf \propto Ri_0^{1-n}. \quad (8.31)$$

In fact, the experimental results with salinity differences, described in section 8.3.2(c) imply that Rf is an increasing function of Ri_0 at low Ri_0 and a decreasing function at high Ri_0 (when $n = \frac{3}{2}$). The point where $n = 1$ corresponds to the simple overall energy argument, with a constant fraction of the energy supply being used for mixing.

Relating this now to the earlier argument, the maximum on figure 8.5 (which is schematic, but has the same form for the grid-stirred and shear-driven experiments) corresponds to the "equilibrium" conditions, where the gradients and fluxes are in balance [equations (8.27) and (8.28)]. If there is a self-balancing mechanism operating in which the rate of energy supply is itself regulated by the mixing it produces [cf. section 8.5.2(a)], then this is the state attained. If there is an excess of mechanical energy and a weak gradient (to the left of the maximum), mixing acts throughout the depth to reduce the gradient and spread out the interface. When the density gradient is the dominant factor (to the right of the maximum), turbulence is suppressed in an interface but can remain unaffected elsewhere, so that it acts to sharpen incipient interfaces. The relation to Phillips's and Posmentier's stability argument becomes clear once we note that, for a fixed rate of kinetic energy supply, Rf is proportional to the buoyancy flux and Ri_0 to the density gradient.

(b) Instability of Waves in a Smoothly Stratified Fluid Next, we consider the mechanisms of instability in a stratified fluid that can lead to local mixing, and thus produce or accentuate nonuniformities of the gradient. All of these involve waves propagating in from the boundaries, with or without a large-scale background shear set up by horizontal pressure gradients. When interfaces are already present, these will be the

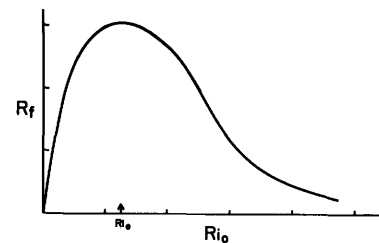


Figure 8.5 Schematic relation between the flux Richardson number Rf and the overall Richardson number Ri_0 for experiments on mixing across a density interface. (After Linden, 1979.) The maximum of the curve corresponds to the "equilibrium" condition.

first regions to become unstable [see section 8.4.1(c)], but it is logical first to describe how such a structure can be set up.

It is only recently that precisely what is meant by the "breaking" of internal waves has been properly investigated (see chapter 9). Some mechanisms are clearly related to localized sources of wave energy at a nearby boundary. Lee waves can be generated by the flow over bottom topography, and when the amplitude becomes large, overturning and the production of "rotors" is possible. When the mean horizontal velocity u varies in the vertical, the "critical-layer" mechanism also leads to the growth of the waves and the local absorption of energy near the level where u equals the horizontal phase velocity of the waves (Bretherton 1966c). Small-scale "jets" attributable to this mechanism have been reported in the ocean.

Nearly always, however, the source of wave energy at a point in the interior of the ocean is not clearly identifiable, and the motion is the result of the superposition of many waves. Energy can then be concentrated in limited regions through two types of interaction. Strong interactions between an arbitrary pair of waves of large amplitude can feed energy rapidly into small-scale forced waves that overturn locally. Resonant interactions are more selective, and require two waves to be such that the sum or difference of their wavenumbers is related to the sum or difference of their frequencies by the same dispersion relation as the individual waves. These are discussed in detail by Phillips (1977a).

Various laboratory experiments have played an important part in illuminating these processes; these (and many other experiments relevant to the subject of this chapter) have been reviewed by Maxworthy and Browand (1975), and by Sherman et al. (1978). McEwan (1971) generated a single low-mode standing wave, and showed that for sufficiently large amplitudes, the original waveform became modulated with two higher modes that formed a resonant triplet with the forced wave. These grew by extracting energy from the original mode until the superposition of the several motions produced visible local disturbances of the smooth gradient, and eventually turbulent patches that were attributed to a shear-breakdown in regions of enhanced density gradient. Orlanski (1972) carried out a similar experiment, but concluded that local overturning was responsible for the production of turbulence. McEwan (1973) used two traveling internal waves of different frequency, interacting in a limited volume of an experimental tank, to examine the local conditions just before breakdown, but he was unable to say definitely whether the primary mechanism for the production of turbulence was shear breakdown or overturning.

During the experiments reported in 1971, McEwan found that patches of turbulence could also be formed

under conditions such that no resonant interaction was predicted [see also Turner (1973a, plate 24)]. More recently, this case has been studied in detail by McEwan and Robinson (1975), who explained it in terms of a "parametric" instability, which is, in fact, another resonant mechanism that had not previously been considered. This one is less selective, and gives rise to waves within a large range of much shorter wavelengths than the forcing wave, as follows. The original long wave produces a modulation of the effective component of gravity acting on shorter waves propagating through the same volume of fluid. When the forcing frequency is nearly twice the frequency of the growing disturbance, energy is fed into this disturbance through a mechanism analogous to that which causes the sideways oscillations of a pendulum to grow when the support is oscillated vertically. The major predictions of the theory, which include an estimate of the amplitude of the forcing wave required for the disturbances to overcome internal viscous dissipation and grow, were accurately verified in a most elegant laboratory experiment.

The application of this mechanism to the ocean has not yet been thoroughly tested, though McEwan and Robinson have extended Garrett and Munk's (1972a) ideas (based on their universal internal wave spectrum) to compute a mean-square slope of the isopycnals, which they deduce is large enough to excite the parametric instability. Much more work on this process is indicated; it certainly seems capable in principle of transferring energy directly from a broad range of large-scale internal waves to much smaller scales and thus creating patches of mixing in an otherwise smoothly stratified ocean.

(c) Mixing Due to Interfacial Shears Once sharp transition regions exist, across which both density and velocity vary markedly, it is easier to understand how local instabilities arise. The now extensive literature in this field has been well reviewed by Maxworthy and Browand (1975), and it will be treated only briefly here.

When the velocity and density profiles are similar, and the shear is gradually increased, a parallel stratified flow becomes unstable when the minimum-gradient Richardson number falls below $1/4$. The fastest-growing instability takes the form of regular Kelvin-Helmholtz (K-H) "billows," with a wavelength that can be predicted knowing the profiles, and that is about six times the interface thickness. Experiments by Thorpe (1971) (see figure 8.6) and Scotti and Corcos (1972) confirmed the linear-stability theory for this case in great detail. On the other hand, when the density profile is much thinner than that for velocity, some wavelengths are unstable at larger values of Ri and interfacial second-mode waves of another type have been observed at Richardson numbers up to 0.7.

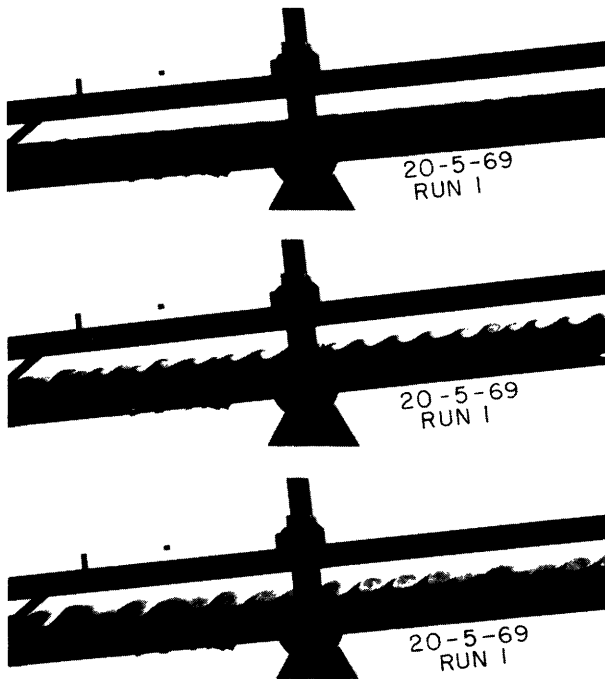


Figure 8.6 The breakdown of an interface in a shear flow to produce an array of Kelvin-Helmholtz billows. (Thorpe, 1971.)

The growth beyond the stage of initial instability has also been studied experimentally [see Thorpe (1973a) for a good review]. When the shear is increased, and then kept constant, the array of billows becomes unstable to a subharmonic disturbance, which leads to a two-dimensional rolling-up and merging of alternate vortices, a process that continues until limited by an energy constraint (as discussed below). Small-scale turbulence is produced by the concentration of vorticity into discrete lumps along the interface, and by gravitational instability within the overturned regions. The system of vortices stops growing, and then collapses, with much horizontal interleaving of mixed regions and a rapid dampening of the turbulence. This leaves behind a smoothly varying, nearly linear mean gradient of density, with thin higher gradient regions superimposed on it. Woods and Wiley (1972) suggested, however, on the basis of measurements in the ocean, that this overturning process should produce a well-mixed layer bounded by sharp interfaces. The implied “splitting” of interfaces to form new regions of high gradient does not seem to be borne out by the subsequent detailed laboratory experiments.

Thorpe (1978a) has reported observations of the mixing across the interface bounding a near-surface layer in a lake under stable conditions. Detailed measurements of temperature profiles as a function of time at one station contain all the features, including overturning and small scale mixing, described for the laboratory experiments. Thorpe concluded that the K-H instability was the dominant mechanism for mixing in

this observation period, and it is likely to be equally important in the ocean under comparable conditions.

The maximum thickening of the interface, due to mixing following the K-H instability, is limited by energy considerations closely related to those set out in section 8.4.1(a). If an initial discontinuity is transformed by this process into linear gradients of velocity and density over the same interfacial depth δ , then equating the changes in kinetic and potential energies gives

$$\delta_{\max} = 2\rho_0 u^2 / g \Delta\rho. \quad (8.32)$$

The process is not perfectly efficient, however, and energy dissipation leads to much smaller limiting values. The numerical factor varies with the initial Richardson number of the interface, but Sherman et al. (1978) suggest using $\delta = 0.3\rho_0 u^2 / g \Delta\rho$ as a typical value.

There are two important implications of this result. First, the instability is self-limiting. Unless the shear is increased, no further instability can occur, because the Richardson number in the thickened state is above that needed for instability. Second, the amount of vertical mixing that K-H instabilities alone can account for is small. Some other mechanism is needed to produce the turbulence in the well-mixed layers, which is essential both to transport heat and salt across them and produce the thinning of the interfaces required before further shear instabilities will be possible.

The shear needed to reduce Ri and so lead to instability at an interface can often be produced by internal waves. When a long internal wave propagates through the ocean, vorticity is concentrated at density interfaces. The sharper the interface, the more unstable it will be (i.e., the smaller the wave amplitude at which billows will form at the crests and troughs). Thorpe (1978b) has recently studied the interaction between finite-amplitude waves and an interfacial shear flow in the laboratory, and has shown that the slope at which breaking occurs can be significantly reduced. Direct visual observations of billows in the ocean generated in this way were made by Woods (1968a), using skin-diving techniques and dye tracers. Those observations had a great influence on subsequent work, by concentrating attention on the need to understand individual mixing events and processes in some detail, rather than always thinking in statistical terms. They also clearly demonstrated the relevance of simple experiments in the ocean and in the laboratory.

Recent, more sophisticated work has confirmed the importance of fine structure as a means for producing mixing in an internal wave field. Eriksen (1978) has described measurements made with an array of moored instruments, which he interprets in terms of large-scale waves “breaking.” (This paper also contains a good summary of the relevant wave theory, and references to related work.) He has shown that the appearance of

local temperature inversions (overturning) is associated with high shears, and that these are dominated by the fine-structure contribution. Moreover, there is a cutoff in the measured values of Ri at $Ri = 1/4$, indicating that regions with lower values of Ri are continuously becoming unstable, and implying some kind of saturation of the wave spectrum (see figure 9.28). Breaking is equally likely at any internal-wave frequency. These deductions were made using differences over 7 m, and it seems probable that the actual mixing events were unresolved at a smaller scale.

(d) Microstructure in Turbulent Patches The breakdown of internal waves by the mechanisms described above leaves behind a turbulent patch of fluid that tends to be thin, but very elongated in the horizontal. Such "blini" or pancakes of turbulence are distributed very intermittently in space and time, and are surrounded by fluid in which the level of fluctuations is very low. Measurements using towed instruments have shown that sometimes the turbulence is "active," i.e., there are both velocity and temperature-salinity fluctuations, but there can also be "fossil turbulence," or T - S microstructure remaining after the velocity fluctuations have decayed. This specialized field can only be mentioned briefly here, though it is important enough to deserve a full-scale review [see Phillips (1977a, chapter 6)]. It has developed somewhat independently, along lines established from the statistical measurements of turbulence properties in laboratory wind tunnels and in the atmosphere, and groups in the U.S.S.R. have been particularly active [see Monin, Kamenkovich, and Kort (1974, chapter 3); Grant, Stewart, and Moilliet (1962); Gargett (1976)]. Recently, other groups have become involved, and more measurements will be summarized in section 8.4.3. In this section we just refer to two results relating to the smallest scales of motion, where the turbulence is isotropic and decaying.

For active three-dimensional turbulence to persist, it is found that the Ozmidov length scale (8.10) must be larger than about 60 times the Kolmogoroff dissipation scale $(\nu^3/\epsilon)^{1/4}$; for typical conditions this implies $L_0 \approx 1$ m. When this is so, the form of the velocity, temperature and salinity-fluctuation spectra can be predicted from the local similarity theory (Batchelor, 1959), using a scaling that does not depend on the buoyancy frequency. When an actively turbulent patch is damped by stratification, however, the form of the fossil (T or S) turbulence is clearly affected by N , and a different scaling is appropriate. The cutoff length scale in the latter case is larger, and in principle the two can be distinguished. The important point made here, and reinforced below, is that fluctuation measurements can only be properly interpreted with a full

knowledge of various other parameters, relating to large as well as small scales.

Osborn and Cox (1972) introduced a method (which is now widely used) for estimating the vertical flux of heat from measurements of temperature fluctuations T' in the dissipation range. They suggested that there is a balance between the production of small-scale variance by turbulent velocities acting in a mean vertical-temperature gradient $\partial\bar{T}/\partial z$ and the destruction of variance by molecular processes acting on sharpened microscale gradients. An effective vertical eddy diffusivity K_z can be defined by

$$K_z = \kappa \overline{(\partial T'/\partial z)^2} (\partial\bar{T}/\partial z)^{-2} = \kappa C, \quad (8.33)$$

where the overbar denotes an average taken over the whole record, and C has been called the Cox number. There is an uncertainty of a factor between 1 and 3 because of the unknown degree of isotropy, but there are also some more fundamental constraints on the use of this idea [e.g., see Gargett (1978)]. Particularly when there are horizontal intrusions, with associated T and S anomalies that can produce correlations between microscale temperature and salinity fluctuations (see section 8.4.3), it is not appropriate to think in terms of a gradient diffusion process based on temperature alone. Stern (1975a, chapter 11) has derived more general thermodynamic relations involving both T and S variances, but these have not yet been properly tested by detailed measurements.

8.4.2 Convective Mixing

(a) Double-Diffusive Instabilities The most dramatic change in the whole field of oceanic mixing has come about through the recognition that molecular processes can have significant effects, even on scales of motion larger than those over which molecular diffusion can act directly. It is not sufficient just to know the net density distribution: the separate contributions of S and T are also important, and when these have opposing effects on the density, the transports of the two properties are quite different, and certainly cannot be described in terms of a single eddy diffusivity. Forty years ago this was unsuspected; twenty years ago a first consequence of unequal transports was recognized but regarded as "an oceanographical curiosity" (Stommel, Arons, and Blanchard, 1956), while in recent years the examples and literature documenting coupled molecular effects has multiplied rapidly.

When temperature and salinity both increase or both decrease with depth, one of the properties is "unstably" distributed, in the hydrostatic sense. The basic fact about double-diffusive convection is that the difference in molecular diffusivities allows potential energy to be released from the component that is heavy at the top, even though the mean density distribution is hydro-

statically stable. Stommel (1962a) was one of the first to recognize that this convective source of energy implies that the potential energy is decreased, and the density difference between two vertically separated regions is increased following mixing—just the opposite to the changes occurring during mechanical mixing (see figure 8.7).

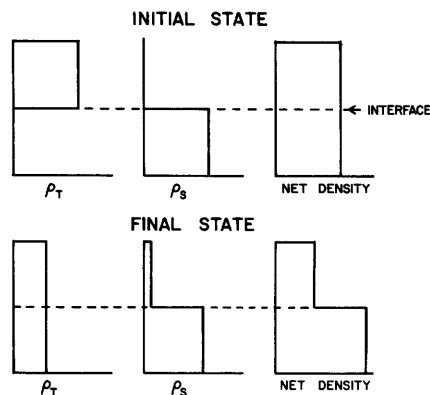
The interaction between theory and laboratory experiments on the one hand, and ocean observations on the other, has played a particularly important role in this field. The early work has been reviewed by Turner (1973a, chapter 8; 1974) and Stern (1975a, chapter 11), and more recent developments by Sherman et al. (1978). It is nevertheless worth repeating a description of two basic experiments that illustrate the different mechanisms of instability in the cases where the temperature and salinity distributions, respectively, provide the potential energy to drive the motion.

When a linear stable salinity gradient is heated from below (Turner and Stommel, 1964; Turner, 1968) the bottom boundary layer breaks down to form a convecting layer of depth d that grows in time as $d \propto t^{1/2}$. The experiments show that there is no discontinuity of density at the top of this layer, i.e., the temperature and salinity steps are compensating. When the thermal boundary layer ahead of the convecting region reaches a critical Rayleigh number Ra_c , it too becomes unstable. The first layer stops growing when d reaches

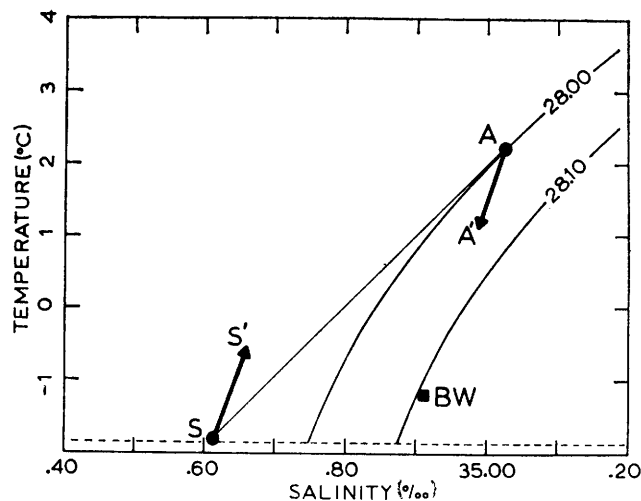
$$d_c = (\nu Ra_c / 4 K_T)^{1/4} B^{3/4} N_s^{-2}, \quad (8.34)$$

and a second convecting layer is formed. Here d_c is the critical depth, $B = -g\alpha F_H / \rho C$ the imposed buoyancy flux corresponding to a heat flux F_H (α being the coefficient of expansion and C the specific heat), and N_s the initial buoyancy frequency of the salinity distribution. Huppert and Linden (1979) recently have extended this work to describe the formation of multiple layers as heating is continued. Linden (1976) used the analog system of salt-sugar solutions to study the case where there is a destabilizing salt (T) gradient partially compensating the stabilizing sugar (S) gradient in the interior. He found that as the density gradients become nearly equal, the properties of the layers depend mostly on the internal properties of the gradient region, with the boundary flux just acting as a trigger. [This analog has been much used for laboratory work, since it eliminates unwanted heat losses, and more experiments using this device will be discussed later. Salt is here the analog of heat, or temperature T , since it has a higher diffusivity than sugar (S).]

This first group of experiments illustrates well an important general consequence of opposing distributions of S and T : smooth gradients of properties are often unstable, and can break up to form a series of convecting layers, separated by sharper interfaces. In the case described, where the hotter, saltier water is



(8.7A)



(8.7B)

Figure 8.7 The changes in the separate concentrations and in the net densities produced by double-diffusion in a two-layer system: (A) schematic diagram of the initial and final properties, with a flux ratio $\beta F_S / \alpha F_T = 0.2$; (B) the water properties in the Greenland Sea on a θ - S correlation diagram. (After Carmack and Aagaard, 1973.) A = Atlantic water, S = Polar water, BW = Bottom water. The double-diffusive flux alters A in direction A' and S in direction S'.

below, the convection is driven by the larger vertical flux of heat relative to salt through the "diffusive" interfaces, which are in turn kept sharpened by the convection in the layers. Many examples of such interfaces are now known in the ocean. They are distinguished from layers formed in other ways [by internal wave breaking, for instance; see section 8.4.1(b)] by the regularity of the steps and the systematic increase of both S and T with depth. For example, Neshyba, Neal, and Denner (1971) have observed such layers under a drifting ice island in the Arctic; they have been found in various lakes that are hotter and saltier near the bottom (Hoare, 1968; Newman, 1976; see figure 8.8), and they occur in various Deeps in the Red Sea (Degens and Ross, 1969).

Now consider the second type of double-diffusive process, that for which the potential energy comes from the salinity distribution (or, more generally, from the component having the *lower* molecular diffusivity). When a small amount of hot, salty water is poured on top of cooler, fresh water, long narrow convection cells or "salt fingers" rapidly form. The alternating upward and downward motions are maintained by the more rapid horizontal diffusion of heat relative to salt, which leaves behind salinity anomalies to drive the motion. The form of motion and the scale was predicted by Stern (1960a) using linear stability theory, and a description of the finite amplitude state has since been given by Linden (1973) and Stern (1975a).

At first sight, there is a very great difference between the finger structure and a series of horizontal convecting layers seen in the "diffusive" case, but Stern and Turner (1969) showed that layers can form in the finger case too. [See also Linden (1978) for a recent experiment of this kind.] A sufficiently large flux of S acting on a smooth gradient of T can cause a deep field of salt fingers to break down into a series of convecting layers, with fingers confined to the interfaces. The mechanism appears to be a "collective instability" (Stern 1969), feeding potential energy from the salt fingers into a large-scale nearly horizontal wave motion that grows in amplitude and leads to overturning. When viewed on the scale of the convecting layers, there is a close correspondence between the two cases; an unstable buoyancy flux across a statically stable interface drives convection in layers, and only the mechanism of interfacial transport differs. Many examples of layering in the ocean due to the fingering process are now known, and they often occur under warm, salty intrusions of one water mass into another. The first observations were made by Tait and Howe (1968, 1971) under the Mediterranean outflow, and a summary of other measurements is given by Fedorov (1976). The direct detection of salt fingers in the interfaces between convecting layers using an optical method (Williams,

1974a, 1975) and conductivity probes (Magnell, 1976) has now given strong support to these ideas.

Another kind of instability that is potentially important is the merging of double-diffusive layers once they have formed. Turner and Chen (1974) and Linden (1976) have shown that this can occur either by the migration of an interface, so that one layer grows at the expense of its neighbor, or by a breakdown of an interface without migration. The possibility of merging implies that one cannot always interpret observed layer scales in terms of the initial mechanism of formation—subsequent events may have changed that scale. Recent theoretical and laboratory work on double-diffusive instabilities, including finite-amplitude effects, has been summarized by Sherman et al. (1978). Much of this has continued to concentrate on one-dimensional effects, though it is difficult to find situations in the ocean where one can be sure that the *formation* of layers and interfaces has been the result of one-dimensional processes. Nevertheless, as is discussed in section 8.4.2(c), the fluxes through such interfaces can probably be adequately described in these terms. The strongest layering is associated with large horizontal gradients of temperature and salinity, and the work that takes this fact explicitly into account will now be presented.

(b) Two- and Three-Dimensional Effects It became clear in early laboratory experiments that layers are readily produced in a smooth salinity gradient if it is heated from the side. Thorpe, Hutt, and Soulsby (1969) and Chen, Briggs, and Wirtz (1971) showed that a series of layers forms simultaneously at all levels by the following mechanism. A thermal boundary layer grows by conduction at the heated wall, and begins to rise. Salt is lifted to a level where the net density is close to that in the interior, and fluid flows away from the wall. The layer thickness is close to

$$l = \frac{\alpha \Delta T}{\beta dS/dz}, \quad (8.35)$$

the height to which a fluid element with temperature difference ΔT would rise in the initial salinity gradient. More recent work has shown that similar layers are formed when the salinity as well as the temperature of the vertical boundary does not match that in the interior, for example, when a block of ice is inserted into a salinity gradient and allowed to melt. Huppert and Turner (1978) have demonstrated that when there is a salinity gradient in the environment, the melt water also spreads out into layers in the interior rather than rising to the surface. This will clearly influence the way icebergs affect the water structure in the Antarctic Ocean, and it also needs to be taken into account when assessing the feasibility of using towed icebergs as a source of fresh water.

Various two-dimensional processes were explored by Turner and Chen (1974) using a tank stratified with opposing vertical gradients of sugar and salt. When an inclined boundary is inserted into a stable "diffusive" system [i.e., one having a maximum salt (T) concentration at the top, and a maximum of sugar (S) at the bottom], a series of layers forms by a closely related mechanism to that of side-wall heating. Both depend on there being a mismatch between conditions at the boundary and in the interior, and again a series of extending "noses" forms, and extends out into the interior. With countergradients in the "finger" sense, disturbances can propagate much more rapidly across the tank in the form of a wave motion, which leads to nearly simultaneous overturning and convection by a mechanism reminiscent of Stern's (1969) collective instability.

The intrusion of one fluid into a gradient of another has been treated explicitly by Turner (1978). The basic intrusion process with which other phenomena can be compared is the two-dimensional flow of a uniform fluid at its own density level into a linear gradient (buoyancy frequency N) of the same property S , for example, salt solution into a salinity gradient. In that case, detailed studies (Maxworthy and Browand, 1975; Manins, 1976; Imberger, Thompson, and Fandry, 1976) show that the intruding fluid remains confined to a thin layer by the density gradient (see figure 8.9). For large Reynolds numbers, there is a balance between inertia and buoyancy forces, and the velocity U of the nose is constant, at

$$U \propto Q^{1/2} N^{1/2}, \quad (8.36)$$

where Q is the volume flux per unit width. At later stages, viscosity dominates and

$$U \propto N^{1/3} Q^{2/3} \nu^{-1/6} t^{-1/6} \quad (8.37)$$

(where ν is the kinematic viscosity), so the velocity decreases in time. These results can be used to describe the flow into the interior of fluid mixed by processes occurring near solid boundaries (section 8.5.4). The related unsteady process, the collapse of a fixed volume of homogeneous fluid into a density gradient, has been studied by Wu (1969a) and Kao (1976); this should model the subsequent spreading of an interior mixed region produced, for example, by breaking waves [section 8.4.1(b)]. Note that relatively sharp density gradients are maintained above and below the intruding fluid (because of the way it distorts the environmental density distribution), so this is another mechanism for producing and extending layered structures. Little research has been done on the corresponding three-dimensional flows, though these are worth further study. More attention should also be paid to the possible effects of rotation in limiting the amount of spreading (cf. Saunders, 1973).

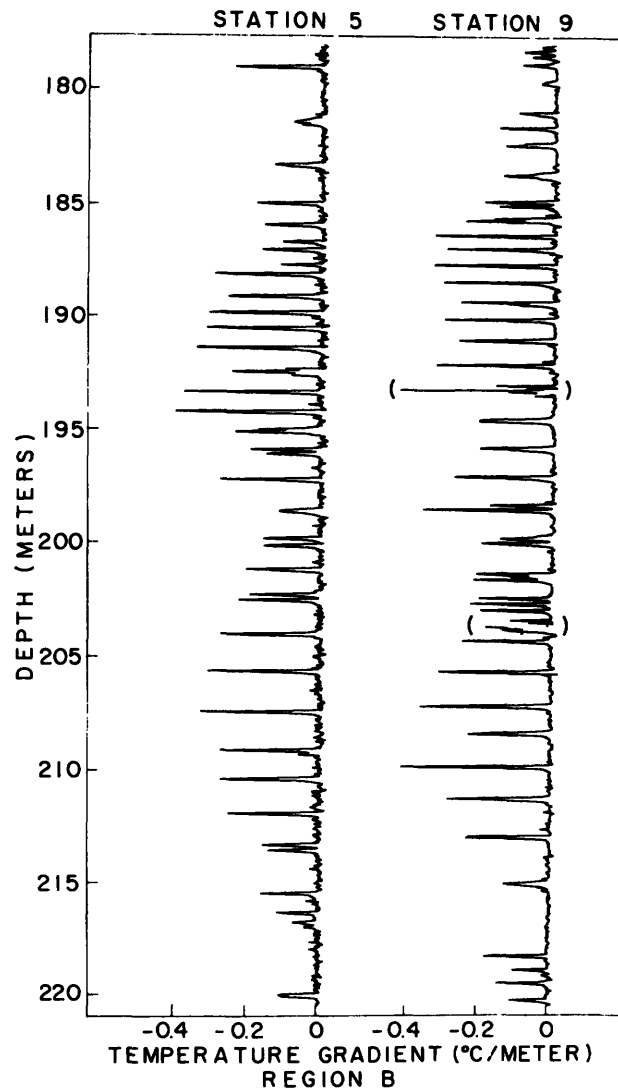


Figure 8.8 Profiles of temperature gradient recorded by Newman (1976) in Lake Kivu, showing a series of homogeneous layers separated by interfaces in which the gradient is much larger.

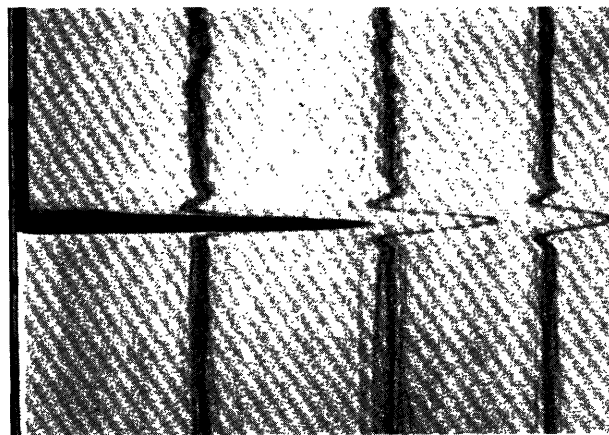


Figure 8.9 A two-dimensional intrusion of dyed salt solution into a salinity gradient at its own density level. (Turner, 1978.) Note the distortion of initially vertical dye streaks, even ahead of the injected fluid.

When the source fluid has different T - S properties from its surroundings, but still the density appropriate to its depth, the behavior is very different. (The laboratory experiments were carried out using a source of sugar in a salinity gradient, but they will be described in terms of the oceanic analog of warm, salty water released into temperature-stratified fresher water.) As shown in figure 8.10, there is a strong vertical convection near the source; this is limited by the stratification, and "noses" begin to spread out at several levels above and below the source. Further layers appear, and the volume of fluid affected by mixing with the input is many times the original volume. Each individual nose as it spreads is warmer and saltier than its surroundings, so "diffusive" interfaces form above and fingers below, and there a local decrease of T or an inversion through each layer. Note too the slight upward tilt of each layer as it extends. This implies that the net buoyancy flux [see section 8.4.2(c)] through the finger interface is greater than that through the diffusive interface, so that the layer becomes lighter and moves across isopycnals. These conclusions have been supported by experiments using a source of salt in a gradient of sugar in which the sense of the interfaces, and the tilt, are just the inverse of those just described. Strong systematic shears are also associated with the layers, and the sense of these motions has been explained in terms of the horizontal density anomalies set up by the net buoyancy flux.

Another geometry of direct relevance to the ocean is a discontinuity of T - S properties in the horizontal over a narrow frontal surface. In the present context, we consider only "fronts" across which the net density difference is small, and neglect rotational effects. [The larger-scale (baroclinic) instabilities that could lead to

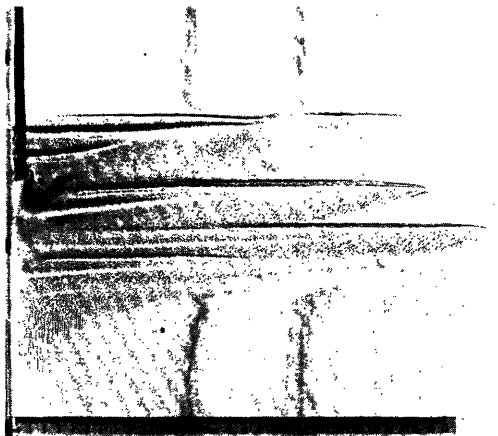


Figure 8.10 The flow produced by releasing sugar solution into a salinity gradient at its own density level. (Turner, 1978.) The gradient and the flow rate are exactly the same as for figure 8.9, but because of the double-diffusive effects, there is now strong convection and mixing near the source, followed by intrusion at several levels.

enhanced horizontal mixing in other circumstances will not be discussed here.] To model this case, Rudnick and Turner (1979) have set up identical vertical density distributions on two sides of a barrier, using sugar (S) in one-half of a tank and salt (T) in the other. When the barrier is withdrawn, a series of regular, interleaving layers develops (figure 8.11) whose depth and speed of advance are both proportional to the horizontal property differences, and therefore increase with depth. The scale is of the form (8.35), where $\alpha \Delta T$ is now the horizontal anomaly across the front (though a rather different energy argument has been used to derive this result).

A general conclusion to be drawn from all the experiments just described is that the formation and propagation of interleaving double-diffusive layers is a *self-driven* process, sustained by *local* density anomalies due to the quasi-vertical transports across the interfaces. Thus, however layers have formed, whether through strictly one-dimensional processes or by interleaving, it is important to understand the mechanism and magnitude of the fluxes of S and T through them.

(c) Double-Diffusive Fluxes through Interfaces

Quantitative laboratory measurements have been made of the S and T fluxes across an interface between a hot, salty layer below a cold, fresh layer. They can be interpreted using an extension of well-known results for pure thermal convection at high Rayleigh number Ra . Explicitly, Turner (1965), Crapper (1975), and Marmorino and Caldwell (1976) have shown that the heat flux αF_H (in density units) is well described by $Nu \propto Ra^{1/3}$, where Nu is the Nusselt number. This may be expressed in the form

$$\alpha F_H = A_1 (\alpha \Delta T)^{4/3}, \quad (8.38)$$

where A_1 has the dimensions of a velocity. For a specified pair of diffusing substances, A_1 is a function only of the ratio R_ρ of contributions of S and T to the density difference

$$R_\rho = \beta \Delta S / \alpha \Delta T, \quad (8.39)$$

where β is the factor relating salinity to density. When $R_\rho < 2$, $A_1 > A \approx 0.1 (g \kappa^2 / \nu)^{1/3}$, the corresponding constant for solid boundaries, and for $R_\rho > 2$, A_1 falls progressively below A as R_ρ increases and more energy is used to transport salt across the interface. As discussed further by Turner (1973a), the empirical form

$$A_1 / A = 3.8 (\beta \Delta S / \alpha \Delta T)^{-2} \quad (8.40)$$

(Huppert, 1971) gives a good fit to the observations.

The salt flux also depends systematically on R_ρ and has the same dependence on ΔT as does the heat flux. Thus the ratio of salt to heat fluxes should be a function of R_ρ alone:

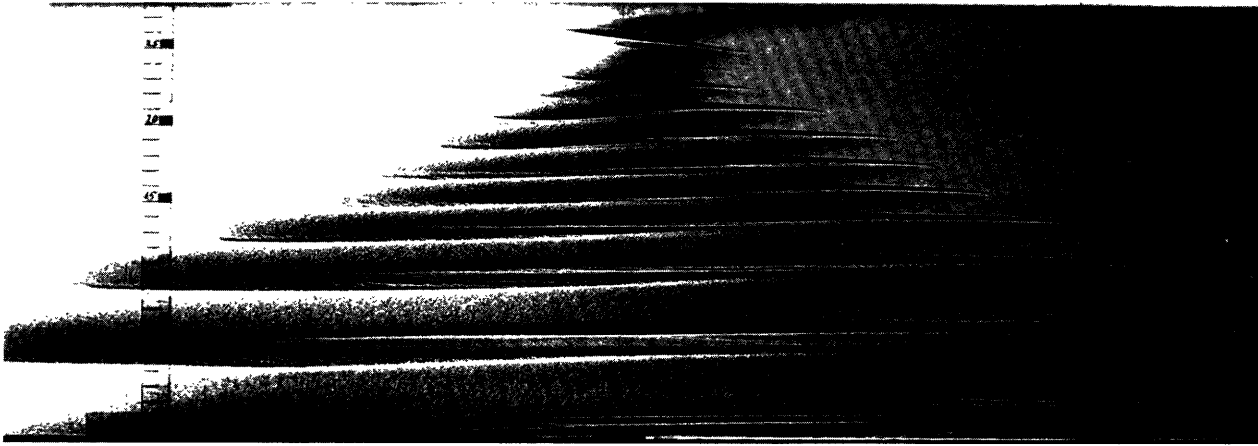


Figure 8.11 A system of interleaving layers produced by removing a barrier separating sugar solution (left) and salt so-

lution (right), which have identical linear vertical density distributions. (Ruddick and Turner, 1979.)

$$R_F = \beta F_S / \alpha F_H = f_*(\beta \Delta S / \alpha \Delta T). \quad (8.41)$$

The first two papers cited above suggest that R_F falls rapidly from unity at $R_\rho = 1$ to 0.15 at $R_\rho = 2$, and then stays constant at $R_F = 0.15 \pm 0.02$ for $2 < R_\rho < 7$. (It must always be less than 1 for energetic reasons, and this implies that the density difference between the two layers will always be increasing in time.) The more recent paper of Marmorino and Caldwell (1976) suggests that the flux ratio can be as high as 0.4 with much smaller heat fluxes, and also gives different values of the normalized heat flux, for reasons that are as yet unresolved. The discrepancy merits further study, since Huppert and Turner (1972) applied the earlier laboratory values to explain the temperature structure of a salt-stratified Antarctic lake, with an accuracy that seemed to make an error of a factor of two unlikely.

Linden and Shirtcliffe (1978) have extended the "thermal-burst" model of Howard (1964a) to calculate fluxes and flux ratios in the two-component case. Transports through the center of the interface are by pure molecular diffusion, while the outer edge becomes intermittently unstable when the Rayleigh number based on its thickness reaches a critical value. [This process had previously been discussed by Veronis (1968a) in a more qualitative way.] The constancy of R_F over a certain range can be predicted by assuming that boundary layers of T and S grow by diffusion to thicknesses proportional to $\kappa_T^{1/2}$ and $\kappa_S^{1/2}$, and then break away together, down to the level where $\alpha \Delta T = \beta \Delta S$. The fluxes will then be in the ratio $\tau^{1/2} = (\kappa_S / \kappa_T)^{1/2}$, a result in reasonable agreement with experiments using both salt-heat and sugar-salt systems. The agreement with the individual flux measurements is much less impressive.

For finger interfaces, the condition for fingers to form in the first place has been examined by Huppert and Manins (1973). They showed that when a hot, salty

layer is placed on a cold, fresh layer (or the equivalent in the analogous system), fingers can form in the interface, as it thickens by diffusion, provided

$$\beta \Delta S / \alpha \Delta T > \tau^{3/2}. \quad (8.42)$$

Since $\tau \approx 10^{-2}$ for heat-salt fingers, only very small destabilizing salinity differences are needed for them to form, and this suggests that salt fingers will be ubiquitous phenomena in the ocean.

Fluxes have also been measured across finger interfaces, and relations like (8.38) and (8.41) are again found to hold. Both the salt flux and the flux ratio are systematic functions of the density ratio, now more conveniently defined in the inverse sense as $R_\rho^* = \alpha \Delta T / \beta \Delta S$. In particular, Turner (1967) found $\alpha F_H / \beta F_S = 0.56$ for heat-salt fingers over the range $2 < R_\rho^* < 10$. This result seems to be confirmed by recent work due to Schmitt (1979) and by the author (unpublished), though a much lower value of the flux ratio obtained by Linden (1973) remains unexplained. No experiments have convincingly achieved values of R_ρ^* very close to 1, where an increase in flux ratio might be expected, but this range could be of great importance for the ocean.

The experiments of Linden (1974) are also of interest. He applied a shear across a finger interface and showed that a steady shear has little effect on the fluxes, though it changes the (nearly square) fingers into two-dimensional sheets aligned down shear. Thus fluxes of S and T will be expected to persist in spite of the shears set up by interleaving motions across a front (figure 8.11). Unsteady shears, on the other hand (i.e., mechanical stirring on both sides of the interface) can rapidly disrupt the interface and decrease the salt flux.

Stern (1975a, 1976) has extended his collective-instability model (in two different ways) to describe the breakdown of fingers at the edge of an interface. He supposes that instability sets in when the salt flux

becomes too large for the existing temperature gradient, a condition that can be expressed in terms of a Reynolds number of the finger motions, and that is achieved first near the edges. This is consistent with a steady state through the interface in which the flux is

$$\beta F_S \sim C(g\kappa_T)^{1/3}(\beta\Delta S)^{4/3}, \quad (8.43)$$

where C is a function of R_ρ^* only when $\tau = \kappa_S/\kappa_T$ is small. When $R_\rho^* < 2$, various laboratory experiments agree in giving $C = 0.1$, and this form is in better accord with experiments than previous expressions, which involved κ_S explicitly. Griffiths (1979) has recently proposed a model based on the intermittent growth and instability (in the Rayleigh-number sense) of the edge of an interface, the model previously applied only to diffusive interfaces. He has been able to predict a flux ratio of about 0.6, and also various properties of the fingers in the interface, including the relation between the width h and length L of the fingers ($h \propto L^{1/4}$ approximately) that was observed by Shirtcliffe and Turner (1970) for sugar-salt fingers.

(d) Multiple Transports through Diffusive Interfaces It is clear from all the results described in the previous section that the "transport coefficients," defined as the vertical fluxes divided by the corresponding mean gradients, are inevitably different for heat and salt when the transports are due to double-diffusive processes acting across interfaces. For a diffusive interface, for example,

$$\frac{K_S}{K_H} = \frac{F_S}{\Delta S} \frac{\Delta T}{F_H} = R_\rho^{-1} \tau^{1/2}. \quad (8.44)$$

The effective "eddy diffusivity" of the driving (unstably distributed) component will always be larger than the driven (see figure 8.7): $K_H > K_S$ in the diffusive case, and $K_S > K_H$ when there are salt fingers. Both T and S are transported down their respective gradients, at different rates, but the inappropriateness of the eddy diffusivity approach becomes obvious when one considers the net density flux. This is transported against the gradient, since the potential energy is decreasing and the density difference tending to increase. Moreover, the largest individual transports occur when the density gradient is weakest, i.e., when $R_\rho \rightarrow 1$.

When there are several different stabilizing salts in a hot, salty layer below a cold, fresh layer, the relative transports of each across the diffusive interface can, however, be usefully described in terms of the ratio of transport coefficients K_i . Turner, Shirtcliffe, and Brewer (1970) suggested that the individual K_i can depend on the molecular diffusivities, and Griffiths (1979) has recently examined this more carefully, both theoretically and experimentally. He has predicted, using

a further extension of Linden and Shirtcliffe's (1978) "intermittent instability" model, that K_1/K_2 should be proportional to $\tau^{1/2} = (\kappa_1/\kappa_2)^{1/2}$ at low total solute-heat density ratios R_ρ^T , and to τ at higher R_ρ^T , where a steady diffusive core dominates. The results are insensitive to the relative contributions of each component to the total density difference.

Experiments at interfacial density ratios between 2 and 4 are consistent with $K_1/K_2 = \tau$, but Griffiths finds an even greater separation of components at higher R_ρ^T , for reasons that are so far unexplained. The results of one of his experiments are shown in figure 8.12. He has also shown that the separation of different salts during transport through a finger interface is relatively unimportant.

These ideas have been tested on a geophysical scale using available data for Lake Kivu, a salt-stratified lake that is heated geothermally at the bottom. As illustrated in figure 8.8, this contains many well-mixed layers separated by diffusive interfaces, and Newman (1976) showed that the upward salt flux, calculated using a heat flux derived from laboratory results, is in satisfactory agreement with the salinity in the river flowing out of the top of the lake. Griffiths has used the geochemical data of Degens et al. (1973) to estimate the fluxes and gradients, and hence K_i , for several ions (potassium, sodium, and magnesium) separately. In the range $R_\rho^T \approx 2.0$, the effective transport coefficients decrease in order of decreasing molecular diffusivity, and the ratios are consistent with the laboratory measurements.

The above results have far-reaching, but as yet hardly explored, implications for the ocean. It is tacitly assumed that a tracer may be used to mark a water mass, and that its changing concentration is a measure of the

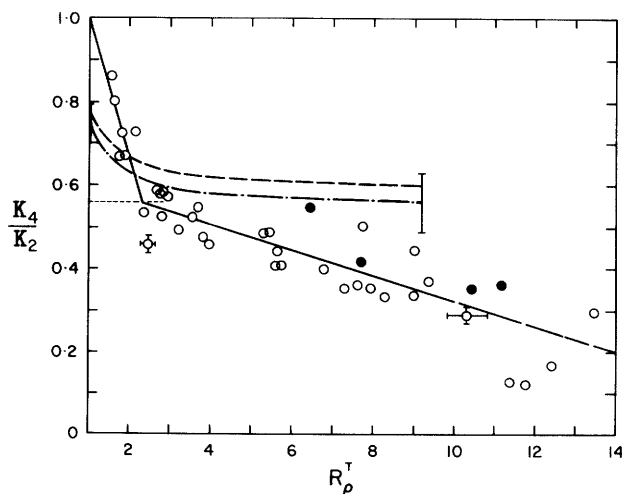


Figure 8.12 The ratio of transport coefficients for magnesium (K_4) and potassium (K_2) measured by Griffiths (1979) across a diffusive interface, with heating below. The ratio of molecular coefficients $K_4/K_2 \approx 0.60$, and the upper curves are Griffiths's theoretical predictions.

“mixing rate” for the water mass as a whole. But if diffusive interfaces are important, the transport of a tracer having a different molecular diffusivity is not necessarily a good indicator of the transport of a major component, much less of heat. In the absence of definite knowledge of the mixing mechanisms operating between the source and the sampling point, a single “eddy diffusivity” must be used with great caution.

(e) Cabbelling and Related Instabilities Another kind of convective instability that can lead to internal mixing depends on the nonlinear-density behavior of sea water. Particularly at low temperatures, the mixing of two parcels of water with the same density but different T - S properties produces a mixture with a greater density than that of the constituents. This will sink, generating additional mixing, and the whole process is called cabbelling (various other spellings appear in the literature). Even when S and T are not quite compensating, so that the density decreases upward, a finite amplitude vertical displacement, followed by mixing, can lead to the effect described.

This possibility was first recognized at the turn of the century. Fofonoff (1956) showed that the formation of Antarctic bottom water is probably influenced by this process, and Foster (1972) has given a good account of the history, as well as a stability analysis for the case of superimposed water masses. He has applied his results to the Weddell Sea, in which the surface is generally colder and fresher than the underlying deep water. When the salinity at the surface increases due to sea-ice formation in the winter, mixtures of surface and deep water may become denser than the deep water, and thus sink through it and contribute to bottom-water formation.

Foster and Carmak (1976b) have since applied related ideas to the explanation of layers at mid-depth in the center of the Weddell Sea. They note that where the T and S gradients are weak and nearly compensating, deep well-mixed layers are formed, and they attribute this to cabbelling. But the sense of the two opposing gradients is just that required for double-diffusive instabilities to produce layers, separated by “diffusive” interfaces. At shallower depths, the gradients are larger and the layers thinner; no cabbelling instability appears to be possible, and layer formation due solely to double-diffusive effects is postulated. A closer study of the conditions separating these regimes would be instructive.

Gill (1973) has shown that when parcels of water are given finite vertical displacements, instabilities can arise due to the different compressibility of sea water at different temperatures and pressures. The compressibility of cold water is generally greater than that of warm, so in the situation discussed above, a cold parcel

displaced downward could in principle become heavier than its new surroundings. The displacements required, however, are rather large, and though the effect may be significant for bottom-water formation (see Killworth, 1977), no evidence has been found that it can influence the formation of layers in the interior, or mixing on a smaller scale.

8.4.3 Observations of Fine Structure and Microstructure

There are now many observations in the deeper ocean in which the influence of the processes described in sections 8.4.1 and 8.4.2 can be identified. Most of these have been made using vertical profiles from lowered or freely falling instruments, with a few significant contributions from towed sensors [see section 8.4.1(d)]. Temperature and salinity fluctuations are the most commonly measured quantities, though small-scale velocity shear measurements are just becoming available (Simpson, 1975; Osborn, 1978).

A useful summary of the observations up to about 1974 has been given by Fedorov (1976) (with extra references in the English translation to mid-1977). He emphasizes the fine structure, or nonuniformities, of vertical gradient associated with a “layer-and-interface” structure, which needs to be known before microstructure measurements in the water column can be understood properly. The strongest layering is found near boundaries between water masses of different origin, and it is most prominent when there is a large horizontal contrast in T - S but a small net density difference. Interleaving motions, with associated temperature inversions, readily develop in these circumstances, and the double-diffusive processes described in section 8.4.2(b) become especially relevant.

Only two recent examples will be cited here: profiles across the Antarctic polar front (Gordon, Georgi, and Taylor, 1977) reveal inversions that decrease in strength with increasing distance away from the front. Joyce, Zenk, and Toole (1978) have made a more detailed analysis of observations in this area, and have concluded that double-diffusive processes are significant. Coastal fronts between colder, fresh water on a continental shelf and warmer, salty water offshore also exhibit strong interleaving (Voorhis, Webb and Millard 1976). More observations and laboratory experiments related to such intrusions have been reviewed and compared by Turner (1978). It must be emphasized that double-diffusive processes can be important even in regions where the mean S increases and T decreases with depth, and both distributions are stabilizing [e.g., off the coast of California (Gregg, 1975)]. Horizontal interleaving organizes the gradients so that double-diffusive convection can act: it is a *self-driven* process, sustained by local density anomalies set up by the quasi-vertical fluxes. In this way double-diffusion

serves both to produce the layering and to dissipate the energy within it. Observations also show (Howe and Tait, 1972; Gargett, 1976) that the density gradient above a warm intrusion is typically much larger than that below, in accord with the laboratory observation of sharp diffusive interfaces above and more diffuse finger interfaces below such an intrusion.

More detailed measurements of microstructure in relation to the fine structure also show the importance of intrusions, though the interpretation of the detailed mechanism involved is sometimes ambiguous. We have already discussed [section 8.4.1(c)] the observations of Eriksen (1978), who related wave-breaking events to the fine structure, so there are certainly some occasions on which shear-generated turbulence is important. Gregg (1975) concluded from T and S microstructure profiles measured in the Pacific that the regions of most intense activity are the upper and lower boundaries of intrusions produced by interleaving, and suggested alternative explanations in terms of shear-generated turbulence and double-diffusive phenomena. The undersides of temperature-inversion layers were found to have the highest level of activity, which we can now attribute to salt fingers. Williams (1976) also found, using thermal sensors mounted on a mid-water float, that the regions of most intense mixing are closely associated with intrusive features, and he was able to distinguish occasions when one or other mechanism was dominant.

Gargett (1976) has shown that higher levels of small-scale temperature fluctuations are invariably found in areas where the vertical profiles of T and/or S have fine-structure inversions. The highest percentage of the sampled water volume was found to be turbulent when the local T and S gradients are in the finger sense. So we come back to the point made by Gargett (1978), and mentioned in section 8.4.1(d); double-diffusive processes, associated with intrusions, are very often important in producing fine structure and microstructure. Thus deductions made on the basis of temperature fluctuations alone, which, moreover, imply that the transport is entirely vertical, are not likely to be valid.

We turn now to examples of the large-scale effects of vertical double-diffusive transports across the boundaries of intrusions. Lambert and Sturges (1977) have shown that the decrease in salinity in and below the core of a warm saline intrusion can be explained in terms of the downward flux of salt in fingers. They observed a series of stable layers separated by finger interfaces, through which the flux (calculated using laboratory results) was sufficient to account for the observed rate of decrease of S with distance. Voorhis et al. (1976) used neutrally buoyant floats to record the change in T and S in the same water mass over a period of days. They found evidence of rapid vertical fluxes of

heat and salt between layers, at different rates consistent with $\alpha F_H/\beta F_S \approx 0.5$, approximately the laboratory value for salt fingers.

Schmitt and Evans (1978) have shown that salt fingers grow rapidly enough to survive even in an active internal wave field. They have calculated salt fluxes for measured profiles of S and T , using laboratory data and assuming that fingers are intermittently active on the high gradient regions. The calculated flux of salt is comparable to the surface input of salt due to evaporation, i.e., they deduce that fingers can account for all the vertical flux in the ocean. Carmack and Aagaard (1973) have given an example of the large-scale importance of vertical transports in the "diffusive" sense. From the changes in S and T in the deep water of the Greenland Sea, they suggest that bottom water is not formed at the sea surface, but by a subsurface modification across an interface between a colder, fresher surface layer of Polar water and a warm salty lower layer of Atlantic water (see figure 8.7B). Their deduced ratio of $K_S/K_T \approx 0.3$, showing that heat is definitely transported faster than salt, supports this view.

Thus, far from being an amusing curiosity, double-diffusive convection is playing a significant, and in some regions dominant, role in the vertical mixing of heat and salt in the world's oceans. Its overall importance relative to other processes such as wave breaking and boundary mixing (reviewed in the following section) has not yet been assessed adequately.

8.5 Mixing near the Bottom of the Ocean

Compared to that in the atmospheric boundary layer, or even the surface layers of the ocean, work on the ocean-bottom layer has been very sparse. The early research, summarized by Bowden (1962), concentrated on shallow seas, but the measurements of heat fluxes through the deep ocean bottom made it desirable to know more about the flows in those regions (Wimbush and Munk, 1970). More sophisticated instruments have now been developed to allow more detailed measurements, but as the proceedings of a recent conference on the subject show (Nihoul, 1977), there is as yet no clear consensus in this field.

8.5.1 Mixing Induced by Mean Currents

Most measurements of the depth of the benthic boundary layer have been referred to the "Ekman depth"

$$h_e = 0.4u_* / f, \quad (8.45)$$

which is the scale appropriate to an unstratified, turbulent flow in a rotating system. A logarithmic layer, described by (8.2), is contained within the lowest part of this, where the stress can be regarded as constant and rotation is unimportant. The Ekman theory also

predicts a veering of the current with height above the boundary.

But the data suggest (in various ways) that this may not be a directly relevant scale, because of the stable stratification of the water column. For example, figure 8.13 shows profiles of θ and S measured by Armi and Millard (1976) on an abyssal plain. The well-mixed layer, bounded by a sharper interface, strongly suggests that this structure has been formed by stirring up the bottom part of the gradient region above (cf. figure 8.1a). This stirring is therefore an "external" mixing process, driven by turbulent energy put in at the boundary. The buoyancy flux associated with the heat flux through the bottom has a negligible effect, except when the speed of the current is very low. The layer depth h in this case is about six times h_e , and the mean depth on different days was correlated with the mean current velocity U . Armi and Millard showed that

$$F = U / \left(g \frac{\Delta\rho}{\rho} h \right)^{1/2},$$

a Froude number, was approximately constant at ~ 1.7 . This led to the hypothesis that the layer depth is controlled by the instability of large-scale waves traveling along the interface. No direct evidence of such a wave-breaking process has been reported, though the temporal variation of layer depth in these and other measurements [see, e.g., Greenwalt and Gordon (1978)] indicate that waves of large amplitude are often present. Note that this Froude-number criterion is closely related to the "constant-overall-Richardson-number" hypothesis used in surface mixed-layer models [sections 8.3.2(a) and 8.3.3].

A different picture has been developed by Weatherly and van Leer (1977), on the basis of their measurements of temperature and current profiles on a continental shelf. Their boundary-layer thicknesses (defined from current profiles) were substantially smaller than (8.45), and they attributed this to the effect of stable stratification. They did, however, observe large changes of current direction in a sense consistent with Ekman veering, particularly when the stratification was large, and they have described their results in terms of a stably stratified turbulent Ekman layer. Relatively few of their profiles had well-mixed layers at the bottom, and even those suggested an advective origin, rather than local turbulent mixing. When the bottom was sloping, and the flow was along the isobaths, the observations contain a systematic increase or decrease of temperature in time, which is consistent with downwelling or upwelling along the slope produced by the Ekman transport.

It seems likely that the difference between these observations and those of Armi and Millard (1976) lies in the much weaker stratification in the deep ocean,

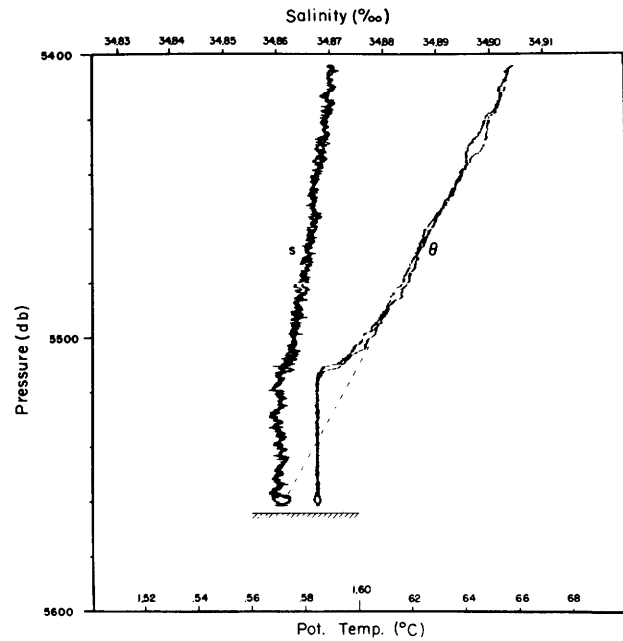


Figure 8.13 Salinity (S) and potential temperature (θ) profiles measured by Armi and Millard (1976) in the middle of the Hatteras Abyssal Plain. The dashed line indicates that the structure could have formed by mixing up a stratified region above the bottom.

and the consequently larger values of F there. But before this can be regarded as certain, more measurements at other sites will be needed. Theoreticians should also look more carefully at the properties of mixed layers shallower and deeper than the Ekman depth, and systematically compare the bottom-layer results with surface mixed layers.

In shallow seas, mixing driven by turbulence produced at the bottom can extend to the surface. This tendency is counteracted by the input of heat at the surface, which produces a stabilizing temperature gradient. Qualitatively, one can see that the larger the current and the shallower the depth, the more likely is the water to be uniformly mixed for a given surface flux [cf. section 8.3.2(d)].

Simpson and Hunter (1974) showed, in fact, that there are marked frontal structures in the Irish Sea, separating well-mixed from stratified regions. The location of these fronts is determined by the parameter h/u^3 , where h is the water depth and u the amplitude of the tidal stream. The choice of this form can be justified using an energy argument, related to that used to obtain (8.21). The relevant dimensionless parameter must include the buoyancy flux B , and is Bh/u^3 . Thus the only extra assumption is that B varies little over the region of interest. Simpson and his coworkers have now extended this model to include the effects of wind stress as well as tidal currents, and find that this has a significant, though less important, influence.

8.5.2 Buoyancy-Driven Bottom Flows

(a) **Turbulent Gravity Currents** The flow of heavier water down a slope under lighter layers is important in many oceanic contexts. The density differences may be due to T and S differences, or to suspended sediment (as in turbidity currents). The velocity of such flows is strongly influenced by the mixing between the current and the water above, and mixing can determine the final destination of the flowing layer. For example, the water flowing out through the Strait of Gibraltar is denser than water at any depth in the Atlantic, but mixing with lighter water near the surface eventually makes its density equal to that of its surroundings, so that it flows out into the interior at middepth (see figure 8.14).

Turner (1973a, chapter 6) has shown how a nonrotating turbulent gravity current can be treated as a special case of a two-dimensional plume, rising vertically through its environment. [This more general problem is also relevant to the disposal of waste water in the ocean, which will not be treated here; see Koh and Brooks (1975) for a review.] The "entrainment assumption," that the rate of inflow u_e is proportional to the local mean velocity u , must be modified to take account of the stabilizing effect of buoyancy normal to the plume edge. Explicitly, it is found that

$$\frac{u_e}{u} = E(Ri_0), \quad (8.46)$$

i.e., the entrainment ratio is a function of an overall Richardson number

$$Ri_0 = \frac{g(\Delta\rho/\rho)h \cos\theta}{u^2} = \frac{A \cos\theta}{u^3}, \quad (8.47)$$

where h is the thickness of the layer, θ the slope, and $A = g(\Delta\rho/\rho)hu$ the buoyancy flux per unit width [cf.

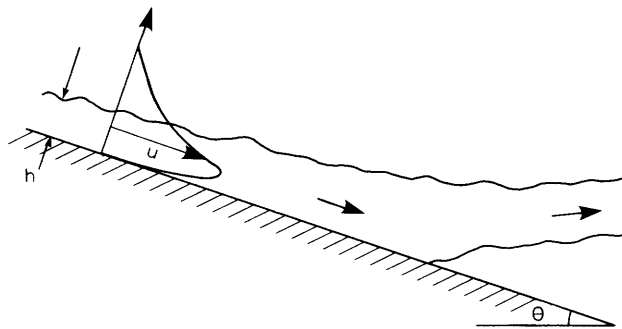


Figure 8.14 Sketch of a steady gravity current on a slope, the edge shown represents the level of most rapid variation of density. The outer part of the velocity profile sketched is linear, and so is the density profile at this level. (Ellison and Turner, 1959.) In stratified surroundings, the plume leaves the slope at a depth given by equation (8.48).

(8.8)]. E is a strong function of Ri_0 (see figure 8.2), and it becomes very small at low slopes.

When θ is small, the stress across the interface is therefore negligible, and the velocity of the layer is determined by friction at the solid boundary. At high slopes, on the other hand, the stress due to entrainment dominates, and in the steady state $u = \text{constant} \propto A^{1/3}$ from (8.47), and the rate of increase of depth with distance $dh/dx = E$. In this state, the turbulence is both generated and used for mixing at the interface, and this flow is thus a good example of the equilibrium "internal"-mixing process referred to in sections 8.2.1 and 8.4.1(a). The profiles of both velocity and density through the outer edge of the interface are observed to be linear, in agreement with an argument equivalent to that which led to (8.27) and (8.28) (figure 8.14).

The results for plumes rising or falling through a stratified environment can also be adapted to describe gravity currents along a slope, just by using the appropriate (smaller) value of E . For example, with a constant slope θ and density gradient (specified by N), the depth at which a two-dimensional current will reach the density of its surroundings and move out into the interior will be

$$Z_{\max} \propto E^{-1/3} A^{1/3} N^{-1}, \quad (8.48)$$

where E is an (empirical) function of θ .

The effects of rotation can be added to these plume theories, and Smith (1975) described a three-dimensional rotating model that fits the observations of outflows from the Norwegian and Mediterranean Seas very well. When entrainment is dominant, rotation makes the flow tend to move along bottom contours, whereas strong bottom friction allows a larger excursion down-slope. Killworth (1977) has discussed and extended rotating two- and three-dimensional models, with the flow on the Weddell Sea continental slope in mind. In order to explain both the depth of penetration and the dilution, he also needed to include the change of buoyancy flux resulting from the increase of thermal expansion coefficient with depth.

(b) **Buoyancy Layers** In a stably stratified fluid, motions along a slope can in principle be set up by diffusion near the solid boundary, which results in the surfaces of constant concentration (of S say) being bent so as to become normal to the slope. This distortion of the density field means that fluid against the boundary will be lighter than that in the interior, and there will be an upslope flow in a thin layer where changes due to advection are balanced by diffusion. Phillips (1970) and Wunsch (1970) showed that with these boundary conditions, the thickness l and upslope velocity w are constant and given by

$$l \sim (\nu\kappa_s)^{1/4}N^{-1/2}, \quad w \sim (\nu\kappa_s)^{1/4}N^{1/2}. \quad (8.49)$$

Under laboratory conditions these are very small, but Wunsch (1970) proposed that (8.49) could be extended to oceanic slopes by using "eddy" values for ν and κ rather than molecular coefficients. With $\nu, \kappa \sim 10^4 \text{ cm}^2 \text{ s}^{-1}$, $l \sim 20 \text{ m}$, $w \sim 5 \text{ cm s}^{-1}$, and more intense mixing will drive a stronger upslope current. There are several difficulties with this interpretation. It is implied that the larger mixing coefficients must be driven by some external mixing process, which is most likely to be associated with currents against the slope. This being so, it seems more appropriate to regard these "mechanical" processes as the cause, not the effect, of the near-slope motions and to investigate directly their effects on mixing. Second, the presence of two stratifying components, in the interior, with compensating effects on the density, changes the behavior markedly. As discussed in section 8.4.2(b) [see also Turner (1974)], counterflows along the slope are then produced, with much larger velocities than in the single-component case. These cannot remain steady, however, and the net result is the formation of a series of layers, extending out into the interior (cf. figure 8.10). When conditions near the slope are quiet, this mechanism could produce enhanced mixing and fine structure, but again it is likely to be overwhelmed by the mixing produced by currents.

8.5.3 Mixing Due to Internal Waves

Internal waves impinging on a sloping boundary can provide enough energy to cause significant mixing. The conditions under which this occurs in a continuously stratified fluid have been convincingly illustrated in the laboratory experiments of Cacchione and Wunsch (1974).

When waves of lowest mode propagate into a wedge-shaped region bounded by a solid sloping boundary and a free surface (or interface), three types of behavior are possible. These depend on the relative magnitudes of the slope β of the boundary and the wave-characteristic slope $\alpha = \sin^{-1}(\omega/N)$, which is the direction of the group velocity, and of the particle motions [see figure 8.15 and Wunsch (1969)]. If $\beta > \alpha$, then energy can be reflected back into the interior. If $\beta < \alpha$, which occurs only at sufficiently high frequencies ω for a given β and stratification N , the horizontal component of the group velocity after reflexion is still directed toward the slope. Energy thus cannot escape backward, and is fed into the corner region. For example, when the deeper layers are stratified, and there is a well-mixed layer above, the amplitude will build up in the thermocline and strong local mixing can occur there. When $\beta = \alpha$, the particle motions become parallel to the slope, and this strong shearing motion becomes unstable to form a series of periodic vortices. Overturning

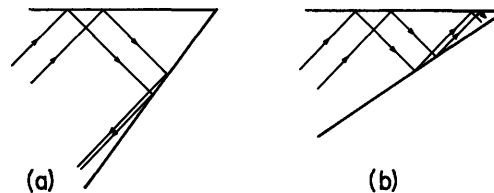


Figure 8.15 Propagation of waves into a wedge of angle β . The angle α that rays make with the horizontal stays constant, so that when $\beta > \alpha$ [case (a)] energy can be reflected, and when $\beta < \alpha$ [case (b)] energy is trapped in the corner. The critical case $\beta = \alpha$ produces strong shearing motions against the slope.

associated with these produces mixed fluid that propagates into the interior as regularly spaced layers all along the slope.

Though there is a suggestion in these and other experiments that the layer spacing is related to the amplitude of the excursion along the slope, they do not provide a definite length scale that can be used for predictions in the ocean. Nor do there yet seem to be any oceanic measurements that are detailed enough to distinguish the structure resulting from this mechanism from other possibilities.

Waves formed on density interfaces can also produce mixing when they approach a sloping boundary. For example, in a fjord that has a well-mixed surface layer and a strong pycnocline at sill depth, Stigebrandt (1976) showed that interfacial waves generated at the sill can propagate toward the landward end, where they break on the sloping shore. Using field data and a laboratory experiment, he described the vertical mixing in the lower layer in terms of this wave-breaking process, followed by the flow of mixed fluid into the interior. Similar observations have been reported by Perkin and Lewis (1978), who concluded that this mechanism probably dominates the transport between the surface and bottom layers of fjords for most of the year.

8.5.4 The Effect of Bottom Mixing on the Interior

There is no doubt that mixing near the bottom is much stronger than it is in the interior of the ocean. Hogg, Katz, and Sanford (1978), continuing a series of measurements near Bermuda initiated by Wunsch (1972a), recently have documented a close relation between the distribution of temperature fine structure and strong currents associated with large eddies near the island. They are cautious about identifying the precise mechanism of interaction (from among those described above, and others not discussed here), but the generation of the structure at the island slope and its decay with distance away from Bermuda is very clear.

Armi (1978) has used the contrast between vertical temperature profiles near topographic features and in the interior of an ocean basin to support one of the mechanisms for vertical mixing discussed by Munk

(1966): that the largest cross-isopycnal mixing occurs in boundary-mixed layers, and that these are then advected into the interior and so influence the structure there as well. The single well-mixed bottom layer discussed in section 8.5.1 and shown in figure 8.13 is characteristic of a smooth bottom on an abyssal plain, but over rougher topography a number of steps is often observed, suggesting bottom mixing at several depths, followed by spreading out along isopycnals that intersect the slope. The horizontal variability of such layering indicates that the process is patchy and intermittent.

The layer structure decays and the profiles become smoother as the water moves out into the interior. The various mechanisms that could play a part at this stage have been discussed in section 8.4. Some layers of water with distinctive T - S properties are identifiable, however, over large distances. Armi (1978) has shown that Norwegian Sea water can be followed as a 20-m-thick layer for over 3000 km into the North Atlantic, and cites this as evidence both for large-scale advection and slow vertical mixing. Carmack and Killworth (1978) have identified a layer with anomalously low T and S characteristics that interleaves along a surface of constant potential density with Antarctic bottom water near the Ross Sea. They also suggest that the sinking of water in the form of plumes along the continental margin, followed by an outflow at mid-depth, is possible nearly everywhere round Antarctica, although water masses that are so clearly distinguishable from their surroundings are rather rare.

In summary, the available evidence supports the view that the bottom of the ocean, particularly the sloping bottom around coasts or topographic features, plays an essential role in the internal-mixing process. Near the topography, the dominant mixing mechanisms are probably mechanical, driven by large-scale currents, though gravity currents can sometimes be important. The main way in which the resulting mixed layers are carried into the interior of the ocean must be by large-scale advection, associated with processes that are nearly independent of the layers themselves. The extra spreading and interleaving due to local horizontal density anomalies [described by equations (8.36) or (8.37)] occur on a longer time scale, though these processes will also affect the final profiles in the interior. Direct vertical mixing driven by internal waves is probably active too, and bottom topography enters here in another way as a mechanism for generating the internal wave field.

The only other regions where the deduced mixing rates are comparable with those at solid boundaries are boundaries between different water masses. The evidence presented in section 8.4.3, for example, shows

that frontal surfaces with large horizontal T and S anomalies but a small net density difference are particularly active. The primary process envisaged in that case is double-diffusive transport in the vertical, producing local density anomalies that drive quasi-horizontal interleaving. Double-diffusive convection can also be significant when water masses with very different T - S properties lie one on top of the other.

We conclude on a cautionary note. Though there have been rapid advances in the observation and understanding of many individual physical processes, particularly in the past 10 years, these have not yet been put together to give a satisfactory, unified picture of mixing in the ocean. We must now seek ways to distinguish between the effects of the diverse vertical and horizontal processes that have been reviewed, and to assess their relative importance in controlling the vertical distributions of temperature and salinity in the ocean as a whole.